Understanding the Fine Structure of Electricity Prices

Hélyette Geman
University Paris Dauphine
& ESSEC Business School

Andrea Roncoroni
ESSEC Business School

- *forthcoming on The Journal of Business* -

Abstract

This paper analyzes the special features of electricity spot prices derived from the physics of this commodity and from the economics of supply and demand in a market pool. Besides mean-reversion, a property they share with other commodities, power prices exhibit the unique feature of spikes in trajectories. We introduce a class of discontinuous processes exhibiting a "jump-reversion" component to properly represent these sharp upward moves shortly followed by drops of similar magnitude. Our approach allows to capture - for the first time to our knowledge - both the *trajectorial* and the *statistical* properties of electricity pool prices. The quality of the fitting is illustrated on a database of major US power markets.

I. Introduction

A decade ago, the electricity sector worldwide was a vertically integrated industry where prices were set by regulators and reflected the costs of generation, transmission and distribution. In this setting, power prices used to change rarely, and in an essentially deterministic manner. Over the last ten years, major countries have been experiencing deregulation in generation and supply activities. One of the important consequences of this restructuring is that prices are now determined according to the fundamental economic rule of *supply and demand*: there is a "market pool" where bids placed by generators to sell electricity for the next day are confronted to purchase orders.

In a parallel way, deregulation of the energy industry has paved the way for a considerable amount of trading activity, both in the spot and derivative markets. Price risk has in particular forced the industry to identify, price and hedge the options granted in energy contracts that have been written for decades.

Given the unique non-storability (outside hydro) of this commodity, electricity prices are much more likely to be driven by spot demand and supply considerations than for any other good, with demand in the short-term market being fairly inelastic. As a result, sizeable shocks in production or consumption may give rise to the price jumps which have been observed since 1998 in various parts in the United States. Leaving aside the California 2000 events which were possibly driven by flaws in market design and wrongdoings on the part of some major players, spike prices have been motivated by disruption in transmission,

generation outages, extreme weather or a conjunction of these circumstances.

Today, an important fraction of the literature on electricity belongs to the economics arena and analyzes deregulated electricity markets from the regulatory viewpoint (see for instance Joskow and Kahn (2001)). It is clear that a proper mathematical representation of spot prices is at the same time a necessary exercise and the cornerstone for the optimal scheduling of physical assets and the valuation of financial and real options in the electricity industry.

Some initial papers on the modeling of power price processes include Deng (1999), Bhanot (2000), Knittel and Roberts (2001), Pirrong (2001), Barone-Adesi and Gigli (2002), Lucia and Schwartz (2002), Barlow (2002), Escribano *et al.* (2002). We extend this literature by proposing a family of stochastic processes meant to represent the *trajectorial and statistical* features displayed by electricity spot prices in deregulated power markets. We also introduce an effective method to identify spikes in historical raw data. In order to empirically investigate the information content of observed power price dynamics, we design a procedure for best fitting our model to market data both in terms of trajectories and moments. Since our focus is an analysis of the empirical properties of electricity prices, we shall solely work under the real probability measure. Yet, our concern is to preserve the Markov property in the view of future developments on derivatives valuation.

The outline of the paper is as follows. Section II discusses the main features of power prices and of the stack function. Section III introduces a class of processes that may encompass prices observed in a variety of regional markets. Section

IV contains the description of data for three major U.S. power markets which exhibit different degrees of mean-reversion and spike behavior. Section V analyzes the statistical methods allowing to select a process matching observed spot prices. Section VI presents empirical results for all models and markets under investigation. Section VII concludes with a few comments and suggestions for future research.

II. The Key Features of Power Prices

Most of the important literature on commodities has focused on storable commodities (see for instance Fama and French (1987)). The same property applies to the specific case of energy commodities, since deregulated power markets were established fairly recently. Bessembinder and Lemmon (2002) build an equilibrium model for electricity forward markets derived from optimal hedging strategies conducted by utilities. They compare in this setting forward prices to future spot prices and show that the forward premium increases when either expected demand or demand risk is high. Geman and Vasicek (2001) empirically confirm Bessembinder and Lemmon's findings and demonstrate, on a U.S. database, that short-term forward contracts are upward biased estimators of future spot prices, in agreement with the high volatility and risk attached to U.S. spot power markets.

Our perspective in this paper is complementary and distinct at several levels. Firstly, we are interested in the modeling of the spot price of electricity, since we

believe that in the wake of deregulation of power markets, a proper representation of the dynamics of spot prices becomes a necessary tool for trading purposes and optimal design of supply contracts. As discussed in Eydeland and Geman (1998), the non-storability of electricity implies the breakdown of the spot-forward relationship and, in turn, the possibility of deriving the fundamental properties of spot prices from the analysis of forward curves. Moreover, as exhibited empirically in markets as different as the Nordpool, the U.K. or the U.S., electricity forward curve moves are much less dramatic than spot price changes.

If we turn to the wide literature dedicated to commodity prices in general, we observe that the convenience yield plays an important role in many cases. The interesting concept of convenience yield was introduced for agricultural commodities in the seminal work by Kaldor (1939) and Working (1949) to represent the benefit from holding the commodity as opposed to a forward contract. Our view is that a convenience yield does not really make sense in the context of electricity: since there is no available technique to store power (outside of hydro), there cannot be a benefit from holding the commodity, nor a storage cost. Hence, the spot price process should contain by itself most of the fundamental properties of power, as listed below.

A first characteristic of electricity (and other commodity) prices is mean reversion toward a level that represents marginal cost and may be constant, periodic or periodic with a trend. Pyndick (1999) analyzes a 127-year period for crude oil and bituminous coal and a 75-year period for natural gas. He concludes that prices deflated (and represented by their natural logarithms), exhibit mean-reversion to

a stochastically fluctuating trend line. In the case of power and with a few years horizon in mind, we propose to represent the diffusion part of the price process as mean-reverting to a deterministic periodical trend driven by seasonal effects. As we shall see, the mean reversion will be more or less pronounced across different markets.

A second feature of the price process, unsurprisingly, is the existence of small random moves around the average trend, which represent the temporary supply/demand imbalances in the network. This effect is locally unpredictable and may be represented by a white noise term affecting daily price variations.

A third and intrinsic feature of power price processes is the presence of so-called spikes, namely one (or several) upward jumps shortly followed by a steep downward move, for instance when the heat wave is over or the generation outage resolved. Since shocks in power supply and demand cannot be smoothed away by inventories, our view is that these spikes will persist beyond the transition phase of power deregulation. The California situation has been widely discussed over the last two years, but many studies neglect to mention that the first event of this nature was totally unrelated to the possible exercise of market power by some key providers: in the ECAR region (covering several Midwestern states of the U.S.A.), prices in June 1998 went to several thousand dollars up from 25 dollars per megawatthour. This spectacular rise was due to the conjunction of a long heat wave, congestion in transmission of hydroelectricity coming from Canada and production outage of a nuclear plant. Within two days, prices fell back to a 50 dollars range as the weather cooled down and transmission capacity

was restored. In Europe, where weather events are usually less dramatic than in the U.S. (and capacity reserves probably higher), prices went from 25 to 500 Euros on the Leipzig Exchange during a long cold spell in December 2001. From an economic standpoint, this phenomenon is illuminated by the graph of the marginal cost of electricity supply, called power stack function (see Eydeland and Geman (1998)). Knowing the characteristics of the different plants in a given region, one can build the supply function by stacking the units in "merit order" from the lowest to the highest cost of production. The part corresponding to low-cost plants (coal-fired or hydro) is fairly flat or with a small upward slope; then the curve reaches a point where there is an exponential price increase corresponding to very expensive units such as "peakers" being activated.

Figure 1 represents the merit order stack for the ECAR region and shows the electricity price as determined by the intersection point of the aggregate demand and supply functions. A forced outage of a major power plant or a sudden surge in demand due to extreme weather conditions would either shift the supply curve to the left or lift up the demand curve, causing in both cases a price jump. These spikes are a major subject of concern for practitioners and a key characteristic of electricity prices. Hence, they deserve to be the subject of a careful analysis.

Figure 1 about here

Following the jump-diffusion model proposed in 1976 by Merton to account for discontinuities in stock price trajectories, a number of authors have introduced a Poisson component to represent the large upward moves of electricity prices;

then, the question of bringing prices down is posed. Deng (1999) introduces a sequential regime-switching representation which may be a good way of addressing the dramatic changes in spot prices; the trajectories produced by the model are however fairly different from the ones observed in the market.

Lucia and Schwartz (2002) examine the Nordpool market and choose not to introduce any jump component in the price process. Data from this market shows that despite the significant part of hydroelectricity in the northern part of Europe, power prices do not have continuous trajectories; for instance, there is a quasi-yearly violent downward jump early April at the end of the snow season when uncertainty about reservoir levels is resolved. This tends to support our view that jump components are hard to avoid when modelling power prices, since they are structurally related to the physical features of this commodity. The class of models presented below is meant to translate the existence of several regimes for electricity prices, corresponding respectively to the quasi-flat and sharply convex parts of the merit order stack. Under the normal regime, the aggregate capacity of generation in the region under analysis is sufficient to meet consumers' demand. In the case of a plant outage, inelastic demand drives spot prices to very high values until the supply problem is resolved, hence the observed large spikes. We can note that in the case of storable commodities (such as oil or wheat), prices are determined not only by supply from existing production and demand for current consumption, but also by the level of inventories. The buffering effect of these inventories does not exist in the case of electricity.

We argue in this paper that the classical setting of continuous-path diffusion

processes does not deliver a viable solution to this problem for reasons linked to trajectorial and statistical features of daily power prices. A jump component should account for the occurrence of spikes through an appropriate jump-intensity function and also explain the significant deviations from normality in terms of high order moments observed in logarithmic prices. Figure 2 compares as an example the empirical distribution in the ECAR market to a normal density with the same mean and variance.

Figure 2 about here

III. The Model

We model the behavior of the price process of one megawatthour of electricity traded in a given pool market.[1] In order to ensure strict positivity of prices and enhance the robustness of the calibration procedure, we represent the electricity spot price in natural logarithmic scale.[2] Throughout the paper, except for the pictures representing trajectories, the term price will refer to "log-price".

The spot price process is represented by the (unique) solution of a stochastic differential equation of the form:

$$dE(t) = D\mu(t)\,dt + \theta_1\left[\mu(t) - E\left(t^-\right)\right]dt + \sigma dW(t) + h\left(t^-\right)dJ(t), \quad (1)$$

where D denotes the standard first order derivative and $f(t^-)$ stands for the left limit of f at time t.

The deterministic function $\mu(t)$ represents the predictable seasonal trend of the price dynamics around which spot prices fluctuate. The second term ensures

that any shift away from the trend generates a smooth reversion to the average level $\mu(t)$. The positive parameter θ_1 represents the average variation of the price per unit of shift away from the trend $\mu(t)$ per unit of time. Note that the speed of mean-reversion depends on the current electricity price level since the constant θ_1 is multiplied by $\mu(t) - E(t^-)$, a difference that may be quite large in electricity markets (in contrast to interest rates or stochastic volatility models for which mean-reversion is classically present). The process W is a (possibly n-dimensional) standard Brownian motion representing unpredictable price fluctuations and is the first source of randomness in our model. The constant σ defines the volatility attached to the Brownian shocks. Note that the instantaneous squared volatility of prices is represented by the conditional second order moment of absolute price variations over an infinitesimal period of time: in the present context, it is the sum of the squared Brownian volatility and a term generated by the jump component (see for instance Gihman and Skorohod (1972)).

The discontinuous part of the process reproduces the effect of periodically recurrent spikes. A spike is a cluster of upward shocks of relatively large size with respect to normal fluctuations, followed by a sharp return to normal price levels. We represent this behavior by assigning a level-dependent sign for the jump component. If the current price is below some threshold, prices are in the normal regime and any forthcoming jump is upward directed. If instead, the current price is above the threshold, the market is experiencing a period of temporary imbalance between demand and supply reflected by abnormally high prices and upcoming jumps are expected to be downward directed.

Jumps are characterized by their time of occurrence, size and direction. The jump times are described by a counting process $N(t)$ specifying the number of jumps experienced up to time t. There exists a corresponding intensity process ι defining the instantaneous average number of jumps per time unit. We choose for ι a deterministic function that we write as:

$$\iota(t) = \theta_2 \times s(t), \tag{2}$$

where $s(t)$ represents the normalized (and possibly periodic) jump intensity shape and the constant θ_2 can be interpreted as the maximum expected number of jumps per time unit.

The jump sizes are modeled as increments of a compound jump process $J(t) = \sum_{i=1}^{N(t)} J_i$. Here the J_i's are independent and identically distributed random variables with common density:

$$p(x; \theta_3, \psi) = c(\theta_3) \times \exp(\theta_3 f(x)), \quad 0 \leq x \leq \psi, \tag{3}$$

where $c(\theta_3)$ is a constant ensuring that p is a probability distribution density and ψ is the maximum jump size. The choice of a truncated density within the exponential family is meant to properly reproduce the observed high order moments.

The jump direction determines the algebraic effect of a jump size J_i on the power price level. It is represented by a function h, taking values $+1$ and -1 according to whether the spot price $E(t)$ is smaller or greater than a threshold

$\mathcal{T}$:

$$h\left(E\left(t\right)\right)=\begin{cases}+1 & \text{if } E\left(t\right)<\mathcal{T}\left(t\right)\\ -1 & \text{if } E\left(t\right)\geq\mathcal{T}\left(t\right)\end{cases}. \tag{4}$$

This function plays an important role in our model for two sets of reasons related to the trajectorial properties of the process and the descriptive statistics of daily price returns. Some authors have proposed to model spikes by introducing large positive jumps together with a high speed of mean reversion; in particular Deng (1999) who was among the first ones to address the specific features of electricity prices. However, models with upward jumps only are deemed to display a highly positive skewness in the price return distribution, in contrast to the one observed in the markets. Other authors model spikes by allowing signed jumps (for instance Escribano *et al.* (2002)), but if these jumps randomly follow each other, the spike shape has obviously a very low probability to be generated. Lastly, another type of solution proposed in particular by Huisman and Mahieu (2001) and Baroni-Adesi and Gigli (2002), is the introduction of a regime-switching model. This representation does not allow the existence of successive upward jumps; moreover, a return to normal levels through a sharp downward jump would require in this case a non Markovian specification. As a consequence, calibrating a regime-switching model is often quite problematic.

In our setting a proper choice of the barrier $\mathcal{T}$ coupled with a high jump intensity can generate a sequence of upward jumps leading to high price levels, after which a discontinuous downward move together with the smooth mean reversion brings prices down to a normal range. Moreover, our representation

has the merit of preserving the Markov property in a single state variable (see Roncoroni (2002)).

Let us observe that general results about stochastic differential equations of the proposed type ensure that equation (1) admits a unique solution (see Gihman and Skorohod (1972)). Hence, the level dependent signed-jump model with time-varying intensity is fully described.

IV. Electricity Data Set

We calibrate the model on a data set consisting of a series of 750 daily average prices compiled from the publication Megawatt Daily for three major U.S. power markets: COB (California Oregon Border), PJM (Pennsylvania-New Jersey-Maryland) and ECAR (East Center Area Reliability coordination agreement). These markets may be viewed as representative of most U.S. power markets both because of their various locations (California, East Coast and Midwestern), because of the different mix of generation (for instance, an important share of hydroelectricity in California) and lastly because of the type of transmission network servicing the region. Moreover, the market design in ECAR and PJM has proved to have functioned properly so far; the choice of the period of analysis (ending in 1999) was meant to leave aside the California crisis and its effects on the COB pool. In terms of price behavior, the COB market is typical of "low-pressure" markets (such as Palo Verde, Mid Columbia, and Four Corners), with high prices ranging between \$90 and \$115 per megawatthour in the examined period. The

PJM market represents a "medium-pressure" market (such as West New York, East New York, and Ercott) with highs between $263 and $412 per megawatthour during that period. Lastly, the ECAR market portrays "high-pressure" markets (such as MAAP, Georgia-Florida Border, North SPP, South SPP and MAIN), experiencing spikes between $1,750$ and $2,950$ dollars per megawatthour.

Figures 3 to 5 depict *absolute* historical price paths in these markets for the period between January 6, 1997 and December 30, 1999.

Figures 3, 4, and 5 about here

As stated earlier, our goal is to adjust our class of processes to both trajectorial features (*i.e.,* average trend, Brownian volatility, periodical component and spikes) and statistical features (*i.e.,* mean, variance, skewness and kurtosis of daily price returns) of historical prices.

In order to start the calibration procedure, we need to detect jumps in the raw market data. The estimation of a mixed jump-diffusion over a discrete sequence $\mathbf{E} = (E_1, ..., E_n)$ of observations may result in an ill-posed problem: standard methods in statistical inference require samples to represent whole paths over a time interval. In the case of discretely sampled observations, there are infinitely many ways a given price variation over a discrete time interval can be split into an element stemming from the continuous part of the process and another from the discontinuous one. Hence, the problem of disentangling these two components on a discrete sample cannot be resolved in a theoretically conclusive way; yet, the situation is better in a continuous time representation, which is our case. All

examined data exhibit excess of kurtosis in the empirical distribution of daily price variations. These changes tend to cluster close to either their average mean or to the largest observed values (see Figure 2). In other words, data suggests that either there is a jump, in which case the variation due to the continuous part of the process is negligible, or there is no jump and the price variation is totally generated by the continuous part of the process. This observation leads us to identify a price change threshold Γ allowing one to discriminate between the two situations. In this order, we extract from the observed data set two important elements of the calibration procedure: the set $\Delta\mathbf{E}^d$ of sampled jumps and the "Γ-filtered" continuous sample path $\mathbf{E}^c$ obtained by juxtaposition of the continuous variations starting at the initial price.[3] A discussion of possible selection schemes in a general mathematical setting may be found in Yin (1988). We include Γ as a parameter to be estimated within the calibration procedure: for each market under investigation, we perform our calibration procedure over different "Γ-filtered" data sets for values of Γ chosen in the set of observed daily price variations. Then, we select the value of Γ leading to the best calibrated model in view of its ability to match descriptive statistics of observed daily price variations. From now on, we suppose a value for Γ has been identified for the market under analysis and input data is described by the corresponding "Γ-filtered" pair $\left(\mathbf{E}^c, \Delta\mathbf{E}^d\right)$.

V. Calibration

We propose a two-step calibration procedure. A first step is the assignment of a specific form for the "structural" elements in the dynamics described in equation (1) and defined as:

- the mean trend $\mu(t)$,
- the jump intensity shape $s(t)$,
- the threshold $\mathcal{T}$ defining the sign of the jump,
- the jump size distribution $p(x)$.

These quantities translate into path properties of the price process.

A second step consists in statistically estimating the four parameters of the selected model, namely:

- the mean reversion force θ_1,
- the jump intensity magnitude θ_2,
- the jump size distribution parameter θ_3,
- the Brownian volatility σ.

The resulting parametric model is fit to the filtered prices by a new statistical method described further on and based on likelihood estimation for continuous-time processes with discontinuous sample paths.

We now illustrate the implementation of this calibration procedure for the ECAR market, propose possible alternatives to the resulting model and defer results and comments to the next section.

A. Selection of the Structural Elements

The mean trend $\mu(t)$ can be determined by fitting an appropriate parametric family of functions to the data set. As mentioned earlier, power prices exhibit a weak seasonality in the mean trend and a sharper periodicity in the occurrence of turbulences across the year. The latter periodicity may be an effective estimate for the one displayed by mean trend: for instance, ECAR market data shows price pressure once a year, during warm season. Some markets display price pressure twice a year, with winter average prices lower than summer average prices (which requires a lower local maximum in the former case). In general, we find that a combination of an affine function and two sine functions with respectively a 12-month and a 6-month periodicity, is appropriate for the U.S. historical data under investigation. We accordingly define the mean trend by a parametric function:

$$\mu(t;\alpha,\beta,\gamma,\delta,\varepsilon,\zeta) = \alpha + \beta t + \gamma\cos[\varepsilon + 2\pi t] + \delta\cos[\zeta + 4\pi t]. \tag{5}$$

The first term may be viewed as a fixed cost linked to the production of power. The second one drives the long run linear trend in the total production cost. The overall effect of the third and fourth terms is a periodic path displaying two maxima per year, of possibly different magnitudes. Observed prices over the three-year period are averaged into a one-year period and bounded from above

by a suitable quantile ν of their empirical distribution. The trend function μ is fitted to the resulting average data by a sequential OLS method providing parameters α, β, γ, δ, ε, and ζ.

We now turn to the identification of the jump intensity shape s. Since spikes occur over short time periods, we select an intensity function exhibiting pronounced convex peaks with annual periodicity. This is meant to reflect the shape of the power stack function which, as shown in Figure 1, becomes very convex (and quasi vertical) at some demand level. Sharp convexity also ensures that the price jump occurrence tends to cluster around the peak dates and rapidly fades away. In this order we choose:

$$s(t) = \left[\frac{2}{1 + |\sin[\pi (t - \tau)/k]|} - 1 \right]^d. \tag{6}$$

Here the jump occurrence exhibits peaking levels at multiples of k years, beginning at time τ.[4] For instance, price shocks concentrating twice a year at evenly spaced dates, with a maximum on August 1, are recovered by the choice $\tau = 7/12$ and $k = 1/2$. The exponent d allows to adjust the dispersion of jumps around peaking times and is included among parameters to be estimated within the calibration procedure. Figure 6 shows intensity functions across different coefficients d and Figure 7 reports a sample of jump times.

Figure 6 about here

Figure 7 about here

We found that in all three examined market the best value for d is 2. We have discussed earlier the introduction of a barrier $\mathcal{T}$ above which all occurring jumps

are downward directed. This threshold may reasonably be defined by a constant spread Δ over the selected average trend:

$$\mathcal{T}(t) = \mu(t) + \Delta. \tag{7}$$

The choice of Δ results from a balance between two competing effects: the greater the value of Δ, the higher the level power prices may reach during pressure periods; the smaller this value, the sooner the downward jump effect toward normal levels. Equally importantly, this number has an impact on the moments of daily price variations. We select Δ in such a way that the corresponding calibrated model generates paths whose average maximal values equal the maximal prices observed in the market under analysis.

The last structural element to be determined is a probability distribution for the jump size. We select a truncated version of an exponential density with parameter θ_3:

$$p(x; \theta_3, \psi) = \frac{\theta_3 \exp(-\theta_3 x)}{1 - \exp(-\theta_3 \psi)}, \quad 0 \leq x \leq \psi, \tag{8}$$

where ψ represents an upper bound for the absolute value of price changes. This distribution belongs to the family described in equation (3), where $c(\theta_3) = \theta_3 / (1 - \exp(-\theta_3 \psi))$ and $f(x) = -x$. The resulting price process is a "special semimartingale", a property required to obtain the statistical estimator proposed in the next section. This completes the first calibration step.

B. Model Parameter Estimation

The issue of estimating discontinuous processes has been the subject of particular attention in the financial econometric literature. The proposed methods mainly draw on the extension of statistical techniques well-established in the case of continuous processes. Beckers (1981), Ball and Torous (1983), and Lo (1988) develop estimators based on moment matching; Johannes (1999) and Bandi (2000) propose non-parametric methods based on higher order conditional moments of instantaneous returns. We choose to focus on maximum likelihood methods. The transition densities they typically require can rarely be computed in analytical terms; in our case, the mixed effect of continuous and jump terms makes the task even more arduous since one has to deal with mixtures of probability distributions. Several numerical devices have been recently proposed in order to overcome these difficulties. Broadly speaking, these methods start by discretizing the process and then computing approximated versions of the targeted transition densities. Pedersen (1995) explores simulation-based schemes, while Andersen *et al.* (2002) make use of auxiliary model approximations. Unfortunately, all these methods suffer from computational complexity because of the necessary double approximation of the process and of the transition densities.

We propose an estimator based on the exact likelihood of the unknown process with respect to a prior process chosen as a reference within the same class. By plugging a piecewise constant sample path agreeing with actual data at the sample dates into this likelihood delivers an approximated likelihood function process. The estimator is provided by the parameter vector maximizing this process over

a suitable domain. This method has two major advantages: first, the analytical form of the exact likelihood function under continuous time observations can be computed for nearly all semimartingales through a generalized version of the Girsanov theorem (see Roncoroni (2002)). Second, the discrete sample estimator converges to the continuous sample one and a well-established estimation theory exists in this latter case. We now explain the details of the procedure.

We compute the log-likelihood function $\mathcal{L}$ for the law of the diffusion process corresponding to an arbitrary parameter vector $\boldsymbol{\theta}$ with respect to the law of the process under a prior reference parameter $\boldsymbol{\theta}^0$. Its exact analytical expression is derived in Appendix A. We decide to choose as starting parameter values $\theta_1 = 0$, $\theta_2 = 1$, $\theta_3 = 1$ which correspond to an absence of drift, a normalized jump intensity and a jump amplitude drawn from a truncated exponential distribution with parameter 1.

The approximate logarithmic likelihood function reads as:

$$\begin{aligned}\mathcal{L}_D\left(\boldsymbol{\theta}\left|\boldsymbol{\theta}^0, \mathbf{E}\right.\right) &= \sum_{i=0}^{n-1} \frac{\left(\mu\left(t_i\right) - E_i\right)\theta_1}{\sigma^2}\left[\Delta E_i^c - D\mu\left(t_i\right)\Delta t\right] - \frac{\Delta t}{2}\sum_{i=0}^{n-1}\left(\frac{\left(\mu\left(t_i\right) - E_i\right)\theta_1}{\sigma}\right)^2 \\ &\quad - \left(\theta_2 - 1\right)\sum_{i=0}^{n-1} s\left(t_i\right)\Delta t + \lg\theta_2 N\left(t\right) \\ &\quad + \sum_{i=0}^{n-1}\left[-\left(\theta_3 - 1\right)\frac{\Delta E_i^d}{h\left(E_i\right)}\right] + N\left(t\right)\lg\left(\frac{1 - e^{-\theta_3\psi}}{\theta_3\left(1 - e^{-\psi}\right)}\right),\end{aligned}$$

where $D\mu\left(t_i\right)$ denotes the first order derivative of μ at time t_i. The first part is a discretized version of the Doléan-Dade exponential for continuous processes. The remaining terms come from the jump part of the process. The log-likelihood function explicitly depends on $\theta_1, \theta_2, \theta_3$, and on the filtered data set $\left(\Delta\mathbf{E}^d, \mathbf{E}^c\right)$, which

in turn is derived from the original market data set $\mathbf{E}$ and the choice of parameter Γ. We maximize this function with respect to $\boldsymbol{\theta}$ over a bounded parameter set $\boldsymbol{\Theta}$ identified through economic interpretation of the model parameters. One may alternatively use Monte Carlo simulated samples to infer a reasonable parameter domain and starting values for the numerical optimization algorithm. We finally obtain a non-linear maximization program of a continuous function over a compact set and classical theorems ensure the existence of a local maximum, which will be our estimate for $\boldsymbol{\theta}^*$.

The constant Brownian volatility over observation dates $0 = t_0 < t_1 < ... < t_n = t$ can be obtained as:

$$\sigma = \sqrt{\sum_{i=0}^{n-1} \Delta \overline{E}\left(t_i\right)^2}, \tag{9}$$

where each summand $\Delta \overline{E}\left(t_i\right)^2$ represents the square of the continuous part $\Delta E^c\left(t_i\right)$ of observed price variations (in a logarithmic scale) between consecutive days t_i and t_{i+1}, net of the mean reversion effect $|\theta_1 \times (\mu\left(t_i\right) - E\left(t_i\right))|$.[5] This estimator converges to the exact local covariance estimator for diffusion processes under continuous time observations (Genon-Catalot and Jacod (1993)). We note that numerical experiments not reported here suggest that a time-dependent volatility does not produce a significant improvement in the estimated process (given the other specifications of our model); moreover in this case a joint estimation of volatility and mean reversion parameters would become necessary.

C. Alternative model specifications

We now consider two models displaying in their discontinuous component features either proposed in existing papers on electricity or that may be envisioned as improvements of some kind.

First, by setting to $+1$ the jump direction function h defined in formula (4), we obtain a restricted model where upcoming jumps are all upward directed and reversion to normal levels is exclusively carried over by the smooth drift component. This upward-jump model represents the classical jump-diffusion extension of the continuous diffusion models proposed over the years by Pilipovich (1997), Barlow (2002), Lucia and Schwartz (2002). All the remaining model specifications are the same as those of our signed-jump model. As a consequence, calibration to market data follows the steps described above, with one major exception: price variations of negative size all enter the estimation of the continuous part of the process (*i.e.,* $\Delta \mathbf{E}^d$ only contains positive jumps).

Alternatively, we may allow the jump intensity function ι defined in formula (2) to be stochastic. In order to account for the dependence of the likelihood of jump occurrence on the price level following upward shocks, we consider the following function of the spot price and time:

$$\iota\left(t, E\left(t^{-}\right)\right) = \theta_2 \times s\left(t\right) \times \left[1 + \max\left(0, E\left(t^{-}\right) - \overline{E}\left(t\right)\right)\right].$$

As in the case of the threshold $\mathcal{T}\left(t\right)$ defining the sign of the jump, we define $\overline{E}\left(t\right)$ as a constant c over the mean trend μ. If the spot price is below the mean trend μ plus this spread c, then intensity is purely time dependent. Each price-unit beyond this boundary amplifies accordingly the time dependent intensity. We

identified that the best intensity function was provided by a choice of c equal to $\Delta/2$ (*i.e.,* an increasing jump occurrence when prices are above the median line between the mean trend $\mu(t)$ and the threshold $\mathcal{T}(t)$). The "max" function ensures that the jump intensity never goes below the "standard level" $\theta_2 \times s(t)$ (that may be viewed as the effect of random outages that strike power plants). This effect is depicted in Figure 8 where stochastic intensity is displayed as a function of time and log-price.

Figure 8 about here

In this signed-jump model, jump occurrence is both time and level dependent. Because all the other model specifications are the same as those in the signed-jump model with deterministic intensity, calibration to market data follows the same steps as described above. The log-likelihood estimator denoted in this case as $\mathcal{L}_R$, becomes slightly more complex:

$$\begin{aligned}\mathcal{L}_S\left(\boldsymbol{\theta}\left|\boldsymbol{\theta}^0,\mathbf{E}\right.\right) &= \sum_{i=0}^{n-1}\frac{(\mu(t_i)-E_i)\,\theta_1}{\sigma^2}\left[\Delta E_i^c - D\mu(t_i)\,\Delta t\right] - \frac{\Delta t}{2}\sum_{i=0}^{n-1}\left(\frac{(\mu(t_i)-E_i)\,\theta_1}{\sigma}\right)^2 \\ &\quad - (\theta_2-1)\sum_{i=0}^{n-1} s(t_i)\max\left(1, E_i-\mu(t_i)-c\right)\Delta t + \lg\theta_2 N(t) \\ &\quad + \sum_{i=0}^{n-1}\left[-(\theta_3-1)\frac{\Delta E_i^d}{h(E_i)}\right] + N(t)\lg\left(\frac{1-e^{-\theta_3\psi}}{\theta_3\left(1-e^{-\psi}\right)}\right).\end{aligned}$$

This expression shows that parameters θ_1 and θ_3 are unaffected by a change in the jump intensity function as the corresponding term can be factored out of the likelihood estimator in absolute scale $\exp(\mathcal{L}_S)$.

VI. Empirical Results

The calibration procedure has been implemented on the U.S. data set described in section IV. We first present results for the signed-jump model, then discuss the quality of our assessments on the data set under analysis and finally conclude on a comparison with the alternative models introduced at the end of Section V.

As mentioned before, the first step is the functional estimation of the structural elements $\mu, s, \mathcal{T}$, and p. The values α, β, γ, δ, ε, and ζ characterizing the average trend function $\mu(t)$ defined in formula (5) are reported in Table I.

Table I about here

The jump intensity shape $s(t)$ is of the form defined in equation (6), with $k = 1$, $\tau = 0.5$, and $d = 2$; this corresponds to a jump occurrence displaying an annual peak strongly clustered around the middle of the year, as observed in all examined markets. The threshold $\mathcal{T}(t)$ is defined by a spread Δ over the deterministic trend $\mu(t)$, where Δ in chosen in the order of 50 percent of the range spanned by the observed log-prices. We observe that both ECAR and PJM reveal no significant linear trend over the three-year sample period, while COB shows a small positive linear trend expressed by the coefficient β.

In all cases, the annual periodicity expressed by the coefficient γ prevails over the semiannual component described by the coefficient δ. Figure 9 represents the average paths for the three regional markets in a joint graph; clearly, the annual component is predominant in the COB market, whereas an additional semiannual

component is significant in the ECAR and PJM markets.

Figure 9 about here

A clear difference between the three markets is represented by the maximum size ψ of daily price variations: for instance, ECAR displays jumps which may be more than three times greater than the maximum value observed in the COB market. In this market, the high percentage of hydrogeneration and the reservoir capacity allow to go through the year - the cold season in particular - with no or mild spikes. In contrast, the PJM and ECAR markets experience both very warm summers and cold winters; this leads to the semiannual periodicity of observed power prices in these regions. However, PJM benefits from a fuel mix in power generation and also from a rich transmission network which has been very efficient since the start of deregulation; hence the less dramatic price spikes observed.

The second step of the calibration procedure is the statistical estimation of parameters $\theta_1, \theta_2, \theta_3, \sigma, \Gamma$, and d**.** The approximated likelihood estimation detailed in the previous section has been implemented by the Levenberg-Marquardt nonlinear maximum search algorithm. Final results are reported in Table II.

Table II about here

All markets exhibit some amount of smooth mean reversion. Note that the value of the reversion force in PJM is significantly greater than ECAR. It is worth emphasizing again that the overall reversion displayed by our model is created by the joint effect of the classical mean reversion and an effect due to the downward jumps. Since ECAR displays more jumps than PJM, the overall reversion effect is

higher than the one observed in the PJM market. This is statistically consistent with the fact that, in PJM, both skewness and kurtosis of daily price increments are lower since the smooth reversion suffices most of the time to ensure return to the average trend. We remark that the expected number of jumps per year is represented by the integral of the calibrated intensity function over one year.

We now turn to the assessment of the quality of the estimated processes. This is performed according to four criteria:

- First, we analyze simulated sample paths together with empirically observed trajectories and make a judgement about the fitting quality of the trajectorial properties.

- Second, we compare simulated moments of the daily increments distribution with the empirical values displayed by each market under investigation.

- Third, we check for the robustness of the procedure by re-estimating simulated sample paths generated by the calibrated model.

- Fourth, we test our model against the most popular representation of electricity spot prices so far, namely a jump-diffusion process with positive jumps only and smooth mean-reversion.

- Fifth, we examine the effect of introducing a price-dependent jump intensity on both trajectorial and statistical properties displayed by the most irregular market in our data set (ECAR).

Figures 10 to 12 show trajectories of the estimated model for the three markets.

Figures 10 to 12 about here

For the purpose of comparison, both historical and sample paths are reported at various scales. The dashed line represents the average mean trend $\mu(t)$. These pictures show that the proposed family of processes is capable to reproduce quite consistently the qualitative features exhibited by power paths in all three examined markets.

Table III reports the mean, standard deviation, skewness and excess of kurtosis of observed and simulated daily price variations.

Table III about here

We see that all statistics of the simulated trajectories are quite satisfactory; there is however a small positive skewness which has no counterpart in the empirical data, suggesting that the reverting component ought to be more pronounced. The most important effect of the signed-jump model is the excellent fit of the leptokurtosicity of the distribution. The relevance of the incorporation of jumps in equity return modelling has been analyzed and exhibited in a number of recent papers of the financial economics literature (see for instance Carr, Geman, Madan, and Yor (2002)). In the case of electricity prices, the non-normality of distributions is widely recognized and kurtosis naturally becomes a key parameter: in these markets where extreme events provide the rational for building small and flexible power plants called peakers, a proper representation of the spikes

and their probability of occurrence (i.e., of the tail of the distribution) is the first requirement a model must satisfy.

We further test the robustness of the estimators by simulating one thousand paths from the estimated process and then using the corresponding increments to reassess the values of the parameters $\theta_1, \theta_2, \theta_3$ and σ. The simulation method is detailed in Appendix B and results are described in Table IV.

Table IV about here

For all estimated models the procedure is satisfactorily stable. We do not report the values for Γ because they are all identical to the original ones. The only slight mismatch occurs for the jump size parameter θ_3 in the case of COB market; this may be due to the very low number of jumps, which makes the estimator sensitive to outliers in the simulated paths. This result is of minor importance, to the extent that the jump component is almost irrelevant for the modelling of COB prices. In general, we conclude that the procedure is not only statistically but also numerically robust.

Returning to the alternative specifications discussed in Section IV.C, we also calibrated the *upward-jump* model with *deterministic* intensity and the *signed-jump* model with *stochastic* intensity to the ECAR market data. For the purpose of comparison, Table V shows the quality assessment of these two models with respect to the benchmark defined by the *signed-jump* model with a *deterministic* intensity.

Table V about here

It is clear that all three models account quite well for the first two moments of daily average prices, with an excess in volatility and positive skewness, however, for the upward-jump model. The signed-jump model with stochastic intensity compared to the one with deterministic intensity slightly improves the value of the skewness, and our view is that this extra-complexity does not bring any decisive improvement. As for the upward-jump model (with deterministic intensity) which is quite popular in the literature on electricity spot price modelling, it generates a kurtosis four times smaller than the real one; this mispecification may translate into a wrong estimation of Value at Risk numbers and have severe consequences in markets where some inefficient plants continue to exist only because of these rare events. In all industries a wrong estimation of reserves leads to harmful consequences.

VII. Conclusion

We have proposed in this paper a family of discontinuous processes featuring upward and downward jumps to model electricity spot prices. Our approach is rooted in the physical properties of electricity, in particular its non-storability, and their consequences on the short-term supply and demand equilibrium in the pool market.

Given the number of state variables that explain power prices in a pool (*i.e.,* temperature, fuel mix, type of transmission network) and their distributional complexity (*e.g.,* plant outages occurrence), we chose a reduced-form representa-

tion in order to get a tractable and efficient tool allowing to handle the random evolution of spot prices and the related management decisions. The calibrated processes exhibit the expected mean reversion property, however in an unevenly pronounced manner depending on the market. All analyzed trajectories show price spikes resulting from momentary imbalance between offered generation and volume of demand. The fitting performed on three major U.S. markets allows to conclude positively on the quality of the model, both in terms of its statistical and trajectorial properties.

References

Andersen, Torben G., Luca Benzoni, and Jesper Lund. 2002. An Empirical Investigation of Continuous-Time Equity Return Models. *Journal of Finance* 57: 1239-1284.

Ball, Clifford A. and Walter N. Torous. 1983. A simplified jump process for common stock returns. *Journal of Financial and Quantitative Analysis* 18: 53-65.

Bandi, Federico. 2000. On the functional estimation of jump-diffusion models. Unpublished Manuscript, University of Chicago.

Barlow, M.T. 2002. A diffusion model for electricity prices. *Mathematical Finance* 12, no. 4: 287-298.

Barone-Adesi, Giovanni, and Andrea Gigli. 2002. Electricity Derivatives. Unpublished Manuscript, National Center of Competence in Research, Università della Svizzera Italiana.

Beckers, Stan. 1981. A note on estimating the parameters of the jump-diffusion model of stock returns. *Journal of Financial and Quantitative Analysis* 16: 127-140.

Bessembinder, Hendrik, and Michael L. Lemmon. 2002. Equilibrium pricing and optimal hedging in equilibrium electricity forward markets. *Journal of Finance* 57: 1347-1382.

Bhanot, Karan. 2000. Behavior of power prices: implications for the valuation

and hedging of financial contracts. *Journal of Risk* 2: 43-62.

Carr, Peter, Hélyette Geman, Dilip Madan, and Marc Yor. 2002. The fine structure of asset returns: an empirical investigation. *Journal of Business* 75, no.2: 305-333.

Deng, Shijie. 1999. Stochastic models of energy commodity prices and their applications: mean reversion with jumps and spikes. Unpublished Manuscript, Georgia Institute of Technology.

Escribano, Álvaro, Juan Ignacio Peña, and Pablo Villaplana. 2002. Modeling electricity prices: international evidence. Working Paper 02-27, Economic Series 08, Departamento de Economia, Universidad Carlos III de Madrid.

Eydeland, Alexander, and Hélyette Geman. 1998. Pricing power derivatives. *Risk* (October).

Fama, Eugene, and Kenneth French. 1987. Commodity futures prices: Some evidence on forecast power, premiums and the theory of storage. *Journal of Business* 60, no.1: 55-73.

Geman, Hélyette, and Oldrich Vasicek. 2001. Forwards and futures contracts on non-storable commodities: the case of electricity, *Risk (*August).

Genon-Catalot, Valentine, and Jean Jacod. 1993. On the estimation of the diffusion coefficient for multidimensional diffusion processes. *Annales de Institut Henri Poincaré* 29, no.1: 119-151.

Gihman, Iosif Il'Ich, and Anatoli V. Skorohod, 1972, *Stochastic Differential Equa-*

tions, Springer-Verlag, NewYork.

Huisman, Ronald, and Ronald Mahieu. 2001. Regime jumps in electricity prices. Working Paper ERS-2001-48-F&A, Erasmus Research Insitute of Management, Rotterdam School of Management, Erasmus University, Rotterdam.

Jacod, Jean, and Albert Shiryaev. 1987. *Limit Theorems for Stochastic Processes.* Springer-Verlag, New York.

Johannes, Michael. 1999. Jumps in interest rates: a nonparametric approach. Unpublished Manuscript, University of Chicago.

Joskow, Paul L., and Edward Kahn. 2001. A quantitative analysis of pricing behavior in Caifornia's wholesale electricity market during summer 2000. Working Paper, AEI-Brookings Joint Center for Regulatory Studies.

Kaldor, N. 1939. Speculation and economic stability. *Review of Economic Studies* 7: 1-27.

Knittel, Christopher R, and Michael R. Roberts. 2001. An empirical examination of deregulated electricity prices. Unpublished Manuscript, Boston University.

Lo, Andrew. 1988. Maximum likelihood estimation of generalized Ito processes with discretely sampled data. *Econometric Theory* 4: 231-247.

Lucia, Julio J., and Eduardo S. Schwartz. 2002. Electricity prices and power derivatives: evidence from the Nordic Power Exchange. *Review of Derivatives Research* 5, 5-50.

Pedersen, Asger Roer. 1995. A new approach to maximum likelihood estimation

for stochastic differential equations based on discrete observations. *Scandinavian Journal of Statistics* 22: 55-71.

Pilipovich, Dragana. 1997. *Energy Risk: Valuing and Managing Energy Derivatives*. McGraw-Hill, New York.

Pindyck, Robert. 1999. The long-run evolution of energy commodity prices. *Energy Journal*, April, IAEE.

Pirrong, Craig. 2001. The price of power: the valuation of power and weather derivatives. Unpublished Manuscript, Oklahoma State University.

Roncoroni, Andrea. 2002. Essays in Quantitative Finance: Modelling and Calibration in Interest Rate and Electricity Markets, PhD Diss., University Paris Dauphine.

Working, Holbrook. 1949. The theory of the price of storage. *American Economic Review* 39**:** 1254-1262.

Yin, Y.Q. 1988. Detection of the number, locations and magnitude of jumps. *Communications in Statistics: Stochastic Models* 4: 445-455.

Footnotes

1. In most markets, this price for date t is defined the day before by the clearing of buy and sell orders placed in the pool.

2. Up to now, negative electricity prices have rarely been observed.

3. If t is a jump date, the continuous part of the path is assumed to be constant between t and the next sample date. Since spikes are rare and typical price variations are much smaller than those occurring during a spike, this simplification does not introduce any significant bias in the estimation procedure.

4. τ is called "the phase" in the language of sinusoidal phenomena.

5. Note that in contrast to classical settings where the mean reversion feature was introduced (*e.g.,* interest rates, stochastic volatility) the difference $\mu(t) - E(t)$ may be quite large in the case of electricity prices. This observation was made in Section III of the paper.

Acknowledgements

This is a revised version of a chapter in the second author's Ph.D. dissertation at the University Paris Dauphine. Both authors wish to thank Alexander Eydeland, Stefano Galluccio, Valentine Genon-Catalot, the Editor (Albert Madansky) and an anonymous referee for helpful comments on earlier versions of the paper. Any remaining errors are our own. The work was financially supported by CERESSEC.

Figure Legends

Figure 1. The power stack function for the ECAR Market.

The generation cost is mildly increasing until a load threshold is reached; then the supply curve exhibits strong convexity.

Figure 2. Empirical Price Returns Distributions vs. Normal Distributions with Equal Means and Variances.

For each market, the empirical density of price returns is reported together with a normal density matching the first two moments. All markets display strong deviations from normality due to the presence of upward and downward jumps.

Figure 3. ECAR Price Path (January 6, 1997 - December 30, 1999).

Spikes concentrate in summer, where prices may rise as high as 2000 U.S. dollars per kilowatt-hour.

Figure 4. PJM Price Path (January 6, 1997 - December 30, 1999).

Spikes concentrate in summer, where prices move up to a level of 400 U.S. dollars per kilowatt-hour.

Figure 5. COB Price Path (January 6, 1997 - December 30, 1999).

Spikes concentrate in summer, where prices rise to values around 100 U.S. dollars per kilowatt-hour.

Figure 6. Time-Dependent Jump Intensity Function.

The time-dependent jump intensity function is designed to concentrated jump occurrence during the warm season. Parameter d drives the degree of cluster.

Figure 7. Sample Jumps of a Time-Dependent Jump Intensity Function.
The time-dependent jump intensity function is designed to concentrated jump occurrence during the warm season. Dotted tags signal the sample jump times of a Poisson process corresponding to the displayed time-dependent intensity function.

Figure 8. Stochastic Jump Intensity Function.
Jump intensity depends on time and electricity price level. If the spot price is below the mean trend μ plus the spread $\Delta/2$, then intensity is only time dependent. Each price-unit beyond this boundary amplifies accordingly the time dependent intensity.

Figure 9. Estimated Average Trends in the Observed Log-Price Paths (January 6, 1997 - December 30, 1999).
PJM and ECAR markets exhibit overlapping periodicities with periods equal to 6 and 12 months. COB essentially displays an annual periodicity.

Figure 10. ECAR Simulated Price Path vs. Empirical Path. Panel (a): absolute scale 0-2500. Panel (b): absolute scale 0-500. Panel (c): absolute scale 0-100.

Figure 11. PJM Simulated Price Path vs. Empirical Path. Panel (a): absolute scale 0-600. Panel (b): absolute scale 0-300. Panel (c): absolute scale 0-100

Figure 12. COB Simulated Price Path vs. Empirical Path. Panel (a): absolute scale 0-175. Panel (b): absolute scale 0-90. Panel (c): absolute scale 0-50.

Tables

Table I: Estimated "Structural" Elements

	Interpretation	ECAR	PJM	COB
α	average log-price level	3.0923	3.2002	2.8928
β	average log-price slope	0.0049	0.0036	0.1382
γ	yearly trend	-0.1300	0.0952	0.1979
δ	6-month trend	0.0292	0.0217	0.0618
ε	yearly shift	0.3325	2.4383	1.7303
ζ	6-month shift	0.7417	0.2907	1.7926
ν	0.7 avg distr. quantile	3.2762	3.3232	3.3586
Δ	jump regime level	2.5000	1.5000	1.0000
ψ	maximum jump size	3.3835	1.6864	1.0169
k	jump periodicity	1.0000	1.0000	1.0000
τ	intensity phase	0.5000	0.5000	0.5000

Note: The electricity log-price model

$$dE(t) = D\mu(t)\,dt + \theta_1\left[\mu(t) - E\left(t^-\right)\right]dt + \sigma dW(t) + h\left(t^-\right)dJ(t),$$

with average trend function

$$\mu(t;\alpha,\beta,\gamma,\delta,\varepsilon,\zeta) = \alpha + \beta t + \gamma\cos\left[\varepsilon + 2\pi t\right] + \delta\cos\left[\zeta + 4\pi t\right],$$

and jump component

$$\begin{aligned}
h\left(t^-\right) &= 1, \text{ if } E\left(t^-\right) < \mu(t) + \Delta;\ -1 \text{ otherwise,} && \text{(Direction)}\\
J(t) &= \sum\nolimits_{i=1}^{N(t)} J_i, \text{ with } J_i \overset{i.i.d.}{\sim} p(x;\theta_3,\psi) \propto e^{\theta_3 f(x)},\ 0 \le x \le \psi, && \text{(Size)}\\
\iota(t) &= \theta_2 \times \left(2/\left(1 + \left|\sin\left[\pi\left(t-\tau\right)/k\right]\right|\right) - 1\right)^2, && \text{(Intensity)}
\end{aligned}$$

is calibrated to a data set including daily observations between January 6, 1997 and December 30, 1999. Observed log-prices over the three-year period are averaged into a one-year period and bounded from above by the 0.7-quantile ν of their empirical distribution. The trend function μ is fitted to the average data by a sequential OLS providing parameters α, β, γ, δ, ε, and ζ. The regime-switching threshold $\mathcal{T}$ is set as a spread Δ over the average trend μ. The jump-size distribution takes values in the interval $[0,\psi]$, where ψ is chosen as the observed maximal daily absolute variation in log-prices. The shape of the jump intensity is described through the parameters k and τ.

Table II: Estimated Model Parameters

	Interpretation	ECAR	PJM	COB
θ_1	Smooth mean-reversion force	38.8938	42.8844	13.3815
θ_2	Max. expected number of jumps	59.5210	63.9301	13.2269
θ_3	Reciprocal average jumpsize	0.3129	0.5016	1.0038
σ	Brownian local volatility	1.8355	1.4453	1.3631
Γ	Jump threshold	0.9200	0.6000	0.6200
$N(1)$	Average number of jumps	9.0000	9.6667	2.0000
n_j	Number of filtered jumps	27	29	6

Note: The model parameters θ_1 (smooth mean-reversion force), θ_2 (maximum expected number of jumps), and θ_3 (reciprocal expected jump size) are selected by an approximated maximum likelihood estimator. The Brownian volatility σ is calculated as a discrete time observation approximation of the standard cumulated covariance estimator on the continuous path obtained by deleting observations of size larger than Γ. The jump threshold Γ is chosen in such a way that the resulting model matches the fourth moment of the daily log-price return distribution. An estimate of the expected number of jumps over one year $N(1)$ is provided by the integral of the intensity function over a one-year period. The quantity n_j denotes the number of observed daily price variations attributed to the jump component of the process according to the selected jump size threshold Γ.

Table III: Moment Matching

	ECAR		PJM		COB	
	EMP	SIMUL	EMP	SIMUL	EMP	SIMUL
Average	-0.0002	-0.0001	-0.0006	0.0000	0.0009	0.0006
Std. Dev.	0.3531	0.3382	0.2364	0.2305	0.1586	0.1121
Skewness	-0.5575	2.1686	0.3949	1.6536	0.1587	0.9610
Kurtosis	21.6833	22.5825	13.1507	14.8429	6.7706	6.5402

Note: For each model estimated by maximum likelihood, descriptive statistics are computed for the empirical versus simulated (after calibration) logarithmic price variations. Statistics include the mean, standard deviation, skewness and excess of kurtosis. Simulations have been performed one thousand times.

Table IV: Parameter Estimation Stability

	ECAR		PJM		COB	
	Original	Re-estim	Original	Re-estim	Original	Re-estim
θ_1	38.8938	37.7559	42.8844	40.0285	13.3815	11.7956
θ_2	59.5210	57.9367	4.1578	4.0188	2.5822	2.4001
θ_3	0.3129	0.2957	0.5016	0.4800	1.0038	1.1897
σ	1.8355	2.1355	1.4453	1.7822	1.3631	1.3882

Note: The parameters $\theta_1, \theta_2, \theta_3$, and σ have been re-estimated by approximated maximum likelihood over 300 simulated paths. Results have been averaged over all samples.

Table V: Moment Matching of Alternative Models in the ECAR Market

	Market	Existing literature	Model I	Model II
	ECAR	Upward-jump det. intensity	Signed-jump det. intensity	Signed-jump stoch.intensity
Average	-0.0002	0.0000	-0.0001	-0.0000
Std. Dev.	0.3531	1.3238	0.3382	0.37821
Skewness	-0.5575	3.5688	2.1686	-0.0119
Kurtosis	21.6833	8.3542	22.5825	28.0288

Note: A comparison between descriptive statistics of empirical data and corresponding statistics is produced for the three models. The first column reports statistics of the ECAR market between January 6, 1997 and December 30, 1999. The second one refers to the standard jump-diffusion model in the existing literature: a smooth mean reverting diffusion with an upward jump component only. The third column relates to our benchmark model (Model I): a jump-diffusion with a deterministic jump intensity; the fourth to a jump reverting diffusion with a stochastic jump intensity (Model II). Each model is estimated by maximum likelihood. Model-generated statistics are computed over a sample of one thousand simulated paths. The simulation algorithm for both deterministic and stochastic jump intensities is detailed in Appendix B.

Appendix A. Likelihood Estimator.

The following proposition is an important result for the estimation of jump processes, both from a theoretical and operational standpoints, and an original contribution of the paper (to our knowledge, at least).

Proposition. Let μ, s, f, c and σ be sufficiently regular functions for the stochastic differential equation (1)-(4) to admit a unique weak solution $E^{\boldsymbol{\theta}}$ for all $\boldsymbol{\theta} = (\theta_1, \theta_2, \theta_3)$ in a compact subset of $\mathbb{R}^3_+$. Let $\mathbf{E} = \{E(t), t_0 \leq t \leq t\}$ be an observed path over the continuous time interval $[t_0, t]$ and $\boldsymbol{\theta}^0 = \left(\theta_1^0, \theta_2^0, \theta_3^0\right)$ a starting parameter set. Then the log-likelihood of observing a realization of the process $E^{\boldsymbol{\theta}}$ with respect to the process $E^{\boldsymbol{\theta}^0}$ is given by:

$$\begin{aligned}
\mathcal{L}\left(\boldsymbol{\theta} \left| \boldsymbol{\theta}^0, \mathbf{E}\right.\right) &= \int_{t_0}^{t} \frac{\left[\mu(u) - E(u^-)\right]\left(\theta_1 - \theta_1^0\right)}{\sigma(u)^2} d\left[E^c\left(u^-\right) - \mu(u)\right] \\
&\quad - \frac{1}{2}\int_{t_0}^{t} \left(\frac{\left[\mu(u) - E(u^-)\right]\theta_1}{\sigma(u)}\right)^2 du \\
&\quad - \left(\frac{\theta_2}{\theta_2^0} - 1\right)\int_{t_0}^{t} s(u)\, du + \left(\lg\theta_2 - \lg\theta_2^0\right) N(t) \\
&\quad + \sum_{u \leq t, \Delta E \neq 0} \left[\left(\theta_3 - \theta_3^0\right) f\left(\frac{\Delta E(u)}{h\left(E\left(u^-\right)\right)}\right) - \lg c(\theta_3) + \lg c\left(\theta_3^0\right)\right],
\end{aligned} \tag{10}$$

where E^c is the path process devoid of its jump component:

$$E^c\left(u^-\right) = E\left(u^-\right) - E_0 - \sum_{s \leq u, \Delta E(s) \neq 0} \Delta E(s), \tag{11}$$

E_0 is the starting point $E(t_0)$, $\Delta E(s)$ is the observed jump size at time s (if any), and $N(t)$ is the number of jumps occurred up to time t.

Proof.

For notational simplicity, we write equation (1) as:

$$dE = (\alpha + \theta_1 \beta)\, dt + \sigma dW + h dJ \tag{12}$$

with $\alpha = D\mu(t)$, $\beta = \mu(t) - E(t^-)$, $h = h(E(t^-))$ and set $t_0 = 0$. We also denote $E(t^-)$ by E^-.

We divide the proof in two steps. First, we compute the semimartingale characteristic triplet $(B_{\boldsymbol{\theta}}, C, \nu_{\boldsymbol{\theta}})$ of the jump-diffusion process E corresponding to a given choice of the parameter $\boldsymbol{\theta}$. Second, we calculate the likelihood by applying a general semimartingale version of the Girsanov theorem (see Jacod and Shiryaev (1987)).

Step I - Since N is independent of J_i for all i, $\mathbb{E}^{\boldsymbol{\theta}}(N(t)) = \iota(t)$, $J_i \overset{i.i.d.}{\sim} p(x;\theta_3)$, and the additive compensator of the purely discontinuous part of the semimartingale E is given by:

$$\begin{aligned}
\nu_{\boldsymbol{\theta}}(dt \times A, t) &= \nu_{\boldsymbol{\theta}}(A,t)\, dt \\
&= \left[\mathbb{E}^{\boldsymbol{\theta}}\left(h\left(E^-\right) d_t\left(\sum_{i=1}^{N(t)} J_i\right)\right)\right] dt \\
&= \left[\theta_2 s(t) \int_{[0,\psi]} dx \left(\mathbf{1}_{A\setminus\{0\}}\left(h\left(E^-\right)x\right) p(x;\theta_3)\right)\right] dt \\
&= \left[\theta_2 s(t) \int_{\mathcal{X}} \frac{x}{h(E^-)} p\left(\frac{x}{h(E^-)};\theta_3\right)\right] dx dt.
\end{aligned}$$

where $\mathcal{X} = \left(\left[0, \frac{\psi}{h(E^-)}\right] \cap A\right)\setminus\{0\}$. Since all coefficients are bounded functions, the process E is a special semimartingale. Consequently, the canonical representation of equation (12) follows by adding and subtracting the compensator $\nu_{\boldsymbol{\theta}}$ to the

jump measure $d\mu_{\boldsymbol{\theta}} = h(t)\, dJ(t)$ and gathering the absolutely continuous terms:

$$dE = \left(\alpha + \beta\theta_1 + \int_{[0,\psi]} d\nu_{\boldsymbol{\theta}}\left(x,t\right) \right) dt + \sigma dW + d\overline{\mu_{\boldsymbol{\theta}}},$$

where $\overline{\mu_{\boldsymbol{\theta}}}$ is a martingale measure under $\mathbb{P}_{\boldsymbol{\theta}}$. From this expression we immediately identify the term of the semimartingale triplet corresponding to $\boldsymbol{\theta}$:

$$B_{\boldsymbol{\theta}}\left(t\right) = \int_0^t \left[\alpha\left(u\right) + \beta\left(u\right)\theta_1 + \int_{[0,\psi]} h\left(E^-\right) x d\nu_{\boldsymbol{\theta}}\left(x,u\right) \right] du, \tag{13}$$

Step II - The semimartingale process under the prior probability $\mathbb{P}^{\boldsymbol{\theta}^0}$ is determined by the characteristic triplet $(B_{\boldsymbol{\theta}^0}, C, \nu_{\boldsymbol{\theta}^0})$. Since:

$$\begin{aligned}
\nu_{\boldsymbol{\theta}}\left(dt \times A\right) &= dt \int_{\mathcal{X}} dx \left\{ \frac{\theta_2}{\theta_2^0} \exp\left[\left(\theta_3 - \theta_3^0\right) f\left(\frac{x}{h\left(E^-\right)} \right) - \left(\lg c\left(\theta_3\right) - \lg c\left(\theta_3^0\right) \right) \right] \right. \\
&\quad \left. \times \theta_2^0 s\left(t\right) \frac{x}{h\left(E^-\right)} \exp\left[\theta_3^0 f\left(\frac{x}{h\left(E^-\right)} \right) - \lg c\left(\theta_3^0\right) \right] \right\} \\
&= \int_{\mathcal{X}} \frac{\theta_2}{\theta_2^0} \exp\left[\left(\theta_3 - \theta_3^0\right) f\left(\frac{x}{h\left(E^-\right)} \right) - \lg c\left(\theta_3\right) + \lg c\left(\theta_3^0\right) \right] \nu_{\boldsymbol{\theta}^0}\left(dt \times dx\right),
\end{aligned}$$

the density of $d\nu_{\boldsymbol{\theta}}$ with respect to $d\nu_{\boldsymbol{\theta}^0}$ is given by:

$$d_{\boldsymbol{\theta}}\left(t,x\right) = \frac{\theta_2}{\theta_2^0} \exp\left\{ \left(\theta_3 - \theta_3^0\right) f\left(\frac{x}{h\left(E^-\right)} \right) - \lg c\left(\theta_3\right) + \lg c\left(\theta_3^0\right) \right\}.$$

By substituting this expression into (13), we see that the drift term under $\mathbb{P}_{\boldsymbol{\theta}}$ can be represented as the sum of the drift term under $\mathbb{P}_{\boldsymbol{\theta}^0}$ and a term denoted as $c_{\boldsymbol{\theta}}\left(t\right)\sigma\left(t\right)$, where:

$$c_{\boldsymbol{\theta}}\left(t\right) = \beta\left(t\right)\left[\theta_1 - \theta_1^0\right]\sigma\left(t\right)^{-1}.$$

Let $\mathbb{P}_{\boldsymbol{\theta}}|_{\mathcal{F}_t}$ be the probability measure induced by $E^{\boldsymbol{\theta}}$ over the path space and restricted to events up to time t. Given the set $\mathbf{E}$ of continuous time observations,

the corresponding density of $\mathbb{P}_{\boldsymbol{\theta}}|_{\mathcal{F}_t}$ with respect to the prior probability $\mathbb{P}_{\boldsymbol{\theta}^0}|_{\mathcal{F}_t}$ is given by the Radon-Nikodym derivative:

$$\left.\frac{d\mathbb{P}_{\boldsymbol{\theta}}}{d\mathbb{P}_{\boldsymbol{\theta}^0}}\right|_{\mathcal{F}_t} = \exp\left\{\int_0^t \left[c_{\boldsymbol{\theta}} dW - \frac{1}{2}c_{\boldsymbol{\theta}}^2 du - \int_{\mathcal{X}} \left(\left(d_{\boldsymbol{\theta}} - 1\right) d\nu_{\boldsymbol{\theta}^0} + \lg d_{\boldsymbol{\theta}} d\mu\right)\right]\right\}.$$

This is a consequence of the Girsanov theorem on measure changes for general semimartingales (see Jacod and Shiryaev (1988)). The first two factors can be written as:

$$\begin{aligned}\exp\left\{\int_0^t \left[c_\theta dW - \frac{1}{2}c_\theta^2 du\right]\right\} &= \exp\left\{\int_0^t \frac{\beta\left(\theta_1 - \theta_1^0\right)}{\sigma^2} d\left[E\left(u\right) - \int_0^u \alpha\left(v\right) dv\right.\right. \\ &\quad \left.\left. - \sum_{s\leq u, \Delta E(s)\neq 0} \Delta E\left(s\right)\right] - \frac{1}{2}\int_0^t \frac{\beta^2\left(\theta_1 - \theta_1^0\right)^2}{\sigma^2} du\right\}.\end{aligned}$$

The third factor is:

$$\begin{aligned}\exp\left\{-\iint \left(d_\theta - 1\right) d\nu_{\boldsymbol{\theta}^0}\right\} &= \exp\left\{-\int_0^t s\left(u\right)\left[\frac{\theta_2}{\theta_2^0}\int_{\mathcal{X}} p\left(\frac{x}{h\left(E^-\right)}; \theta_3\right) dx\right.\right. \\ &\quad \left.\left. - \int_{\mathcal{X}} p\left(\frac{x}{h\left(E^-\right)}; \theta_3^0\right) dx\right] du\right\} \\ &= \exp\left\{-\left(\frac{\theta_2}{\theta_2^0} - 1\right)\int_0^t s\left(u\right) du\right\},\end{aligned}$$

where use the property $\int_{\mathcal{X}} p\left(\frac{x}{h(E^-)}; \theta\right) dx = 1$.

The fourth factor is:

$$\begin{aligned}\exp\left\{\int_0^t \int_{\mathcal{X}} \lg d_{\boldsymbol{\theta}} d\mu\right\} &= \exp\left\{\int_0^t \int_{\mathcal{X}} \left[\left(\theta_3 - \theta_3^0\right) f\left(\frac{x}{h\left(E^-\right)}\right) - \lg c\left(\theta_3\right) + \lg c\left(\theta_3^0\right)\right] d\mu\right. \\ &\quad \left. + \left(\lg\theta_2 - \lg\theta_2^0\right)\int_0^t \int_{\mathcal{X}} d\mu\right\} \\ &= \exp \sum_{u\leq t, \Delta E(u)\neq 0} \left[\left(\theta_3 - \theta_3^0\right) f\left(\frac{\Delta E\left(u\right)}{h\left(E^-\right)}\right) - \lg c\left(\theta_3\right) + \lg c\left(\theta_3^0\right)\right] \\ &\quad + \left(\lg\theta_2 - \lg\theta_2^0\right) N\left(t\right),\end{aligned}$$

where the last equality stems from the relation between the process and the measure representation of any marked point process. Substituting the expressions of α and β leads to the log-likelihood function (10). *Q.E.D.*

Appendix B. Simulation Algorithm

Monte Carlo simulations of trajectories described in equation (1) serve three purposes. First, they provide a starting value $\boldsymbol{\theta}^0$ for the maximum likelihood search algorithm. This is accomplished by sampling trajectories for several parameter sets until we find one whose corresponding simulated paths show qualitative features comparable with those displayed in the empirical observations. Second, sample trajectories allow one to judge upon the qualitative performance of the calibrated model and to compute simulated moments of various orders for the daily price variations. This is used for moment matching in the last step of the calibration procedure. Third, simulations provide a robustness analysis of the estimation procedure: parameters of a calibrated model can be re-estimated over simulated paths. The closer to the original values are the re-estimated ones, the more robust the likelihood estimation procedure is. We detail a simulation algorithm for sampling a path defined by equation (1). The Euler approximation of the stochastic differential equation (1) over a discrete set of evenly-spaced sample times $t_1, ..., t_N$ is:

$$E_{k+1} = E_k + D\mu\left(t_k\right) \times \Delta + \theta_1 \left[\mu\left(t_k\right) - E_k\right] \times \Delta + \sigma\sqrt{\Delta}\mathcal{N} + h\left(t_k\right) \times \mathbf{1}_i \times J,$$

where $\mathcal{N}$ is a sample from a standard normal distribution and J is a sample from $p\left(\cdot, \theta_3\right)$. The function $\mathbf{1}_i$ is either 1 or 0 according to whether t_i is, or is not, a jump time of the process. In order to sample jump times of a point process with non constant deterministic intensity, we may first simulate jump times of a constant intensity Poisson process and then use a variation of the

"acceptance-rejection" method to make sure that these are statistically identical to the required sample set of times. More precisely, on a given horizon $[0, T]$, we generate inter-arrival times ε_i until their sum exceeds T. Each ε_i is a sample from an exponential distribution with parameter $\iota^* = \max_{t\in[0,T]} \iota(t)$. Candidate jump times τ'_k are defined by approximating each $\sum_{i=1}^{k} \varepsilon_i$ to the closest element in the set of sample times $\{t_1, ..., t_N\}$. For each k, we draw a uniform random variable U_k on $[0, \iota^*]$ and accept τ'_k if $U_k \leq \iota(\tau'_k)$, otherwise reject it. The set of selected times is hence a sample sequence $(\tau_1, ..., \tau_n)$ of the jump times for a compound jump process with intensity function $\iota(t)$. Consequently, $\mathbf{1}_i = 1$ if $t_i = \tau_k$, for some $k = 1, ..., n$. This completes the description of the simulating algorithm for any calibrated solution of equation (1).

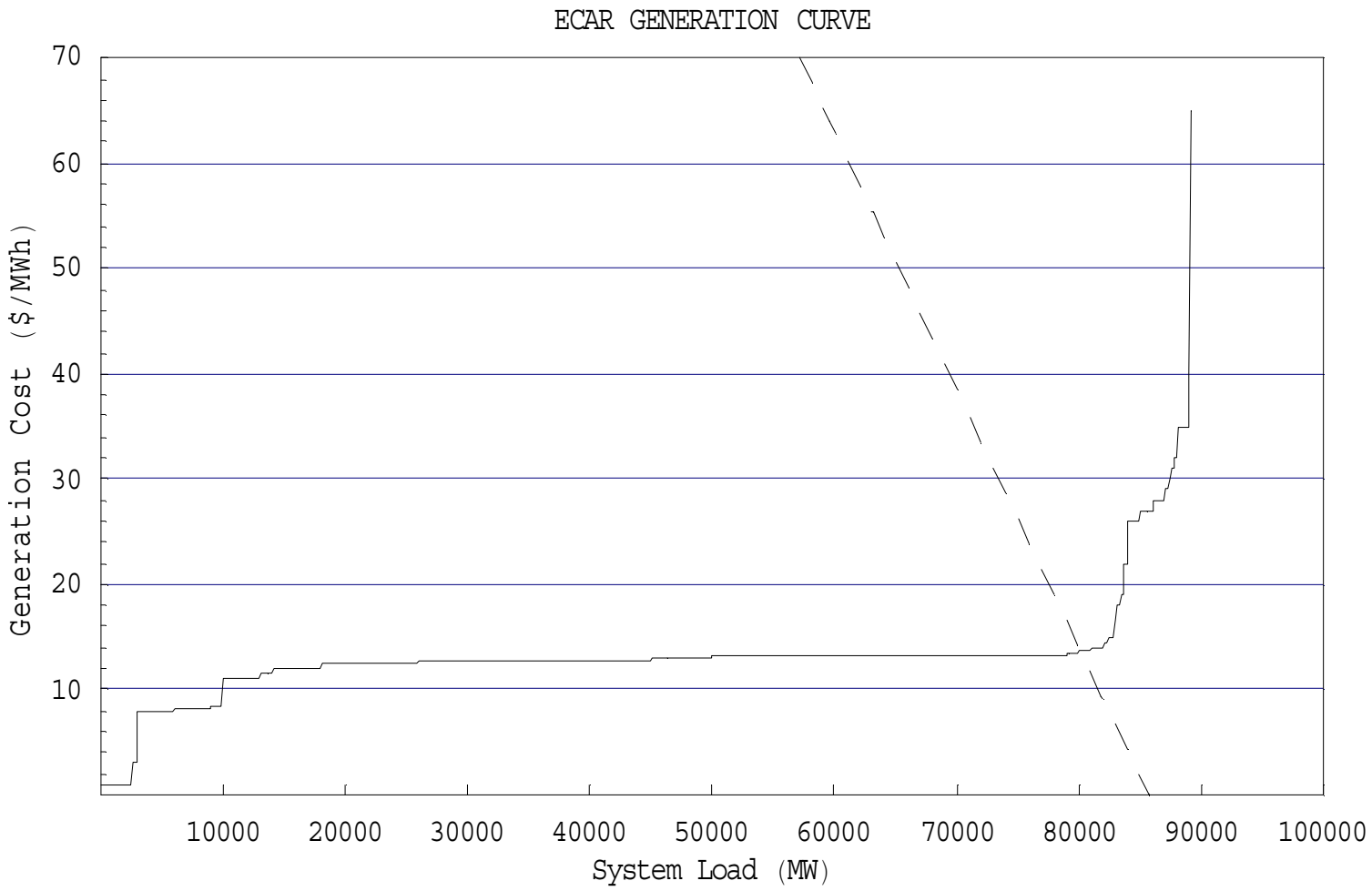
ECAR GENERATION CURVE
70
60
50
40
30
20
10
Generation Cost ($/MWh)
10000
20000
30000
40000
50000
60000
70000
80000
90000
100000
System Load (MW)

Figure 1

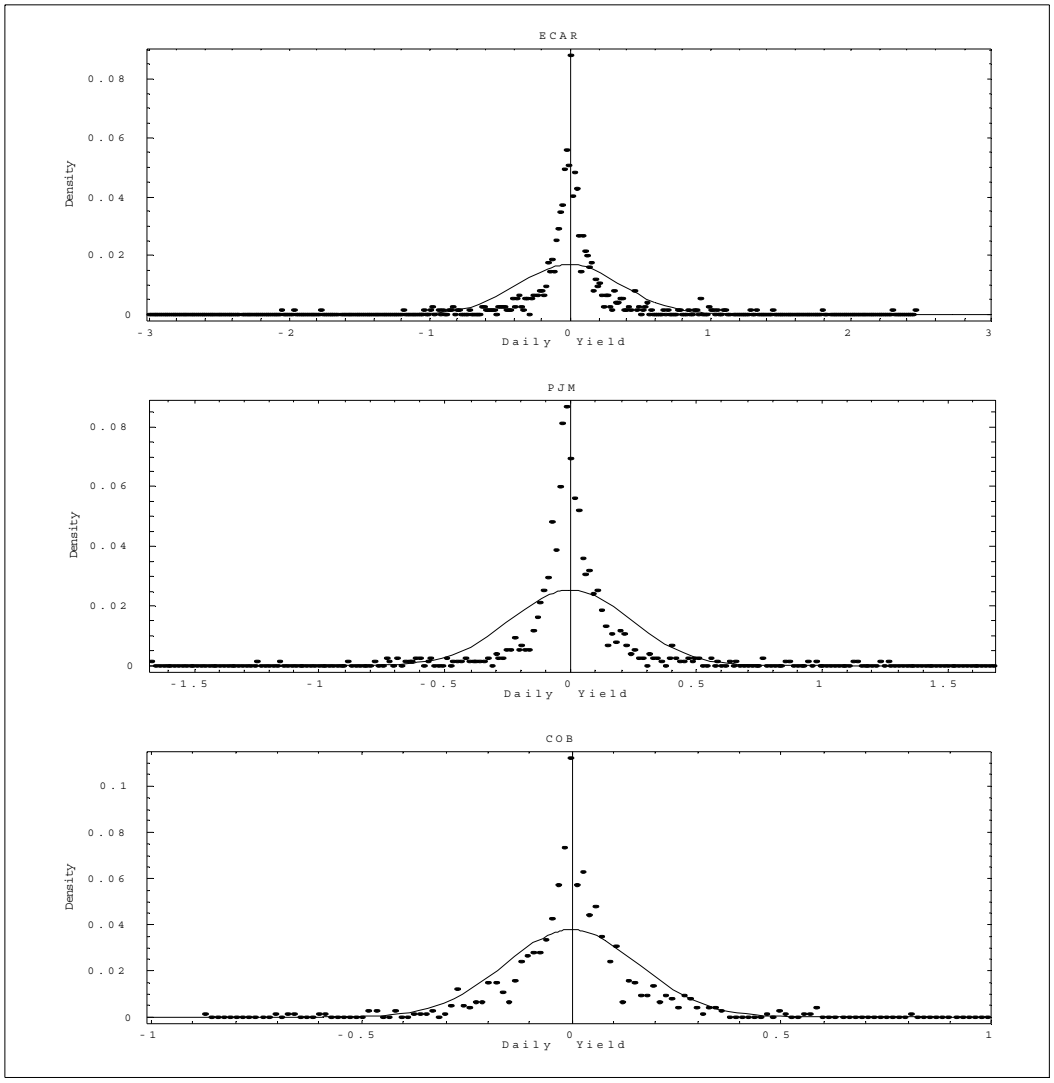
ECAR
Density
0.08
0.06
0.04
0.02
0
-3
-2
-1
0
1
2
3
Daily Yield
PJM
Density
0.08
0.06
0.04
0.02
0
-1.5
-1
-0.5
0
0.5
1
1.5
Daily Yield
COB
Density
0.1
0.08
0.06
0.04
0.02
0
-1
-0.5
0
0.5
1
Daily Yield

Figure 2

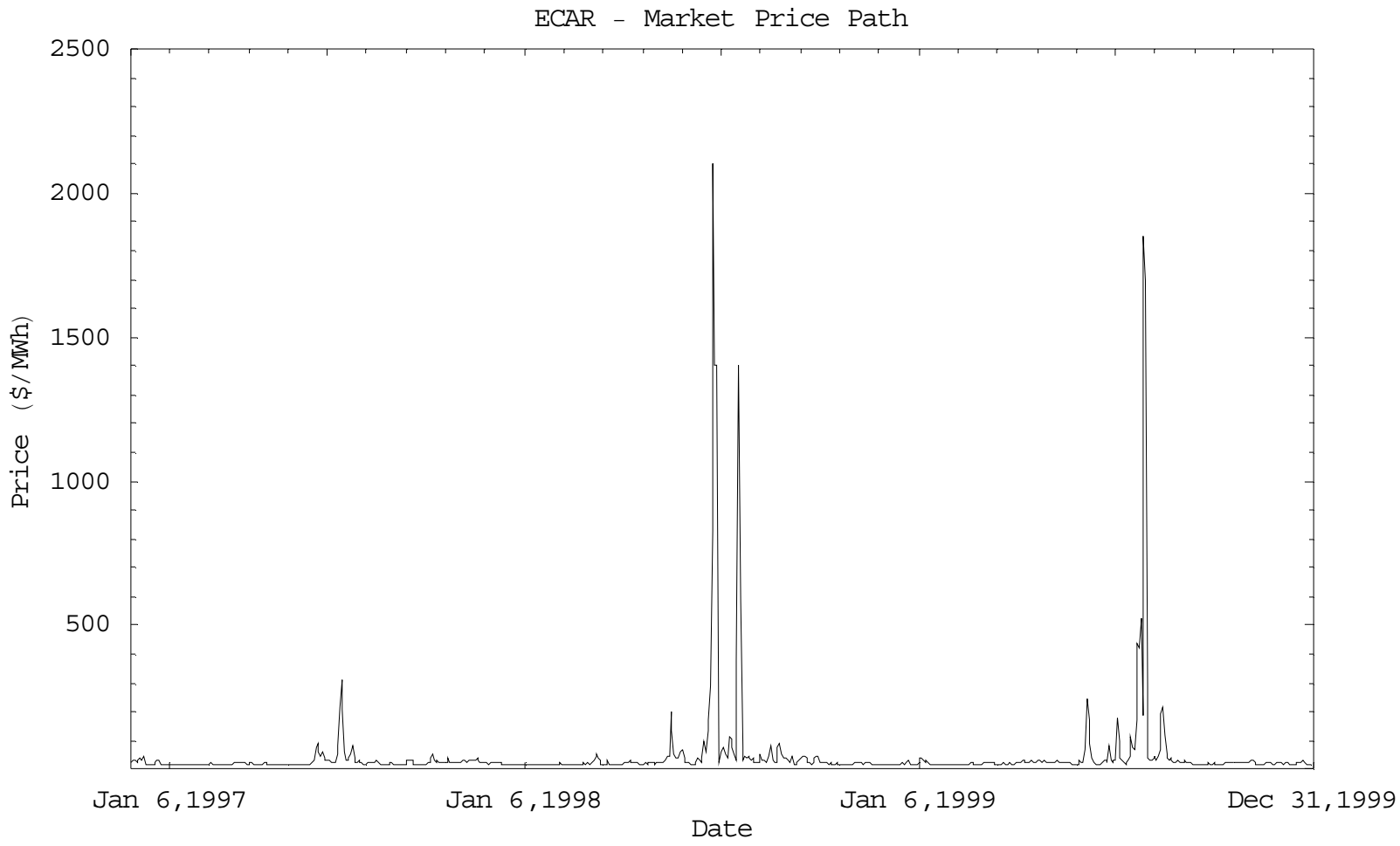
ECAR - Market Price Path
2500
2000
1500
1000
500
Price ($/MWh)
Jan 6,1997
Jan 6,1998
Jan 6,1999
Dec 31,1999
Date

Figure 3

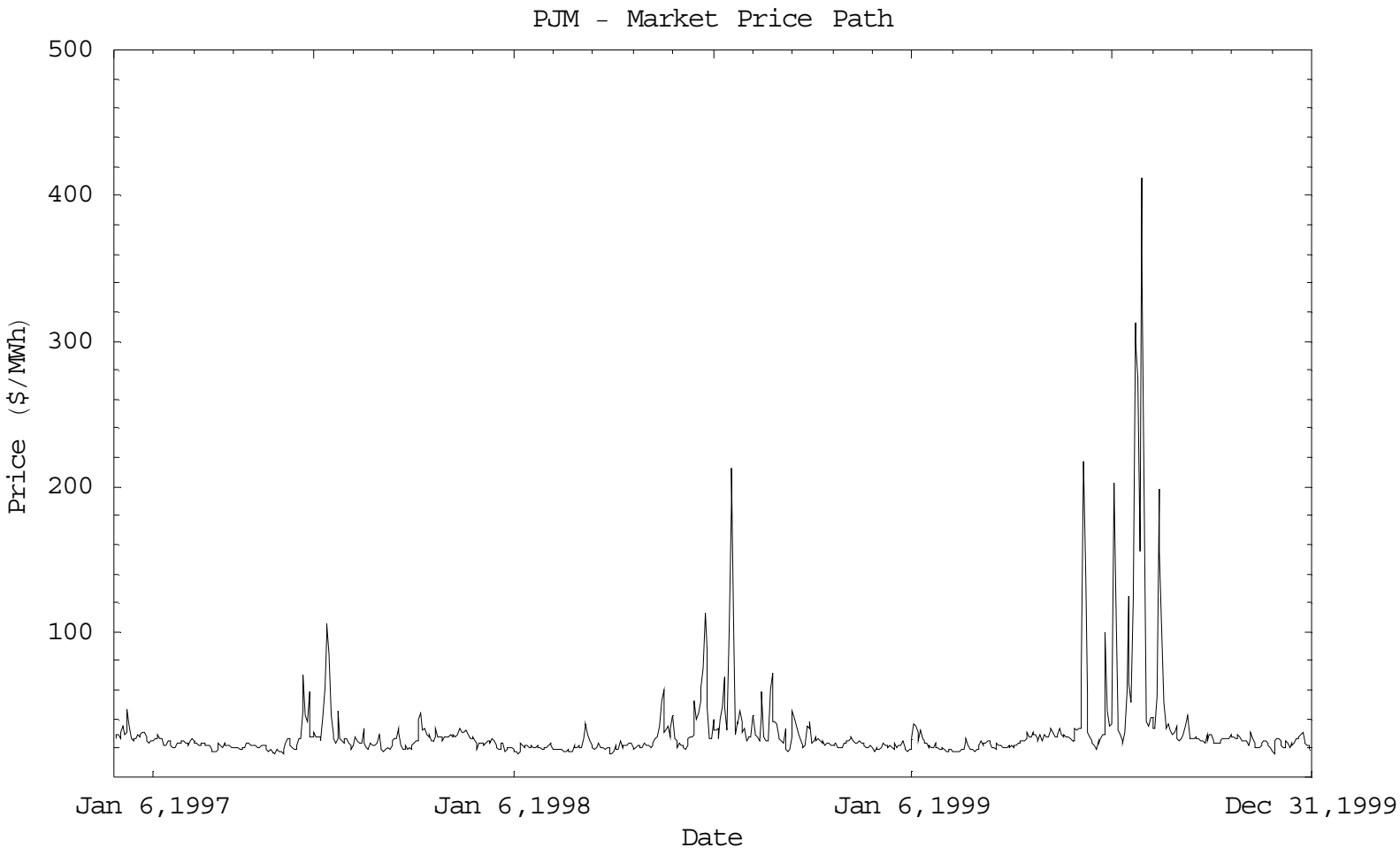
PJM - Market Price Path
500
400
300
200
100
Price ($/MWh)
Jan 6,1997
Jan 6,1998
Jan 6,1999
Dec 31,1999
Date

Figure 4

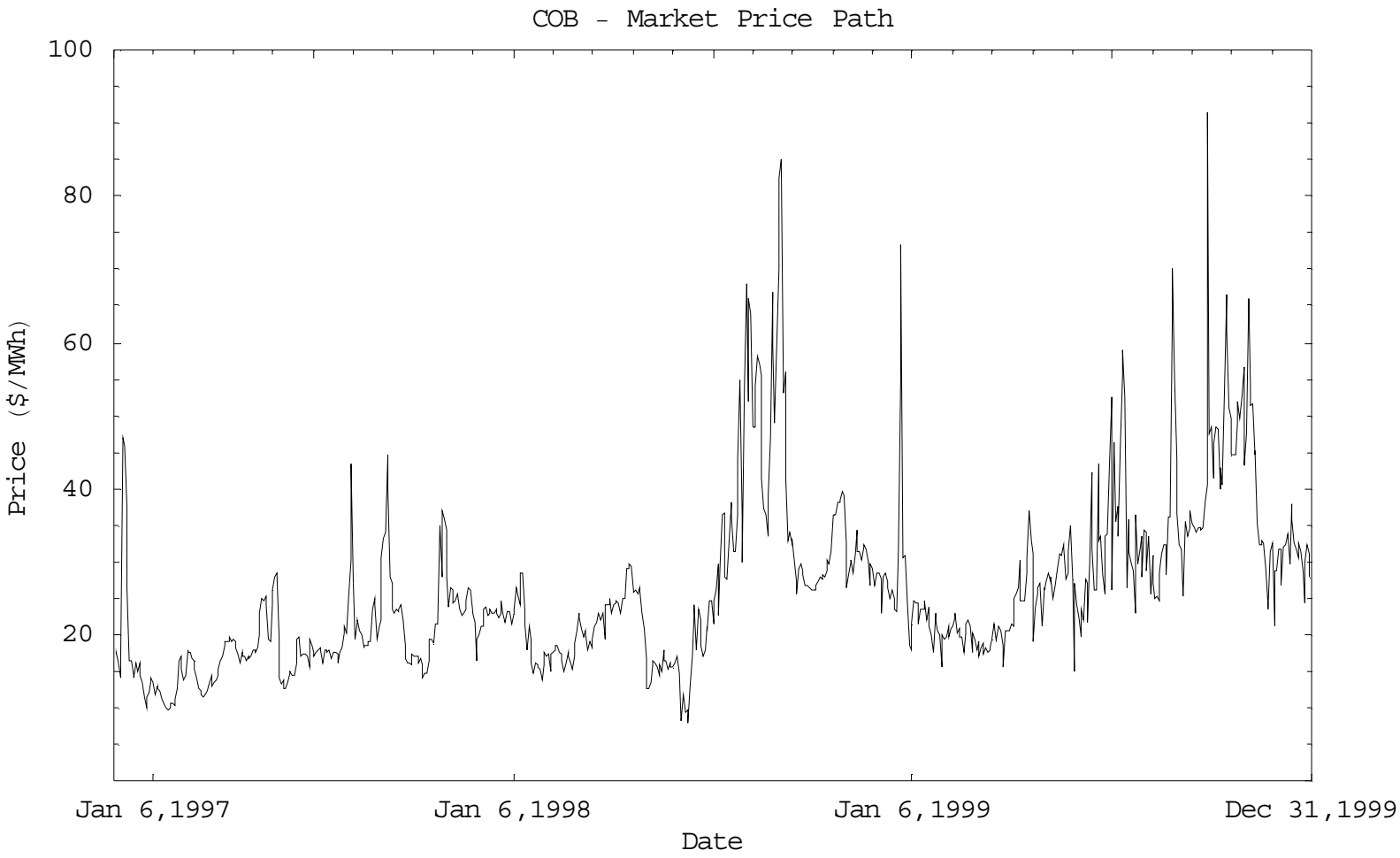
COB - Market Price Path
100
80
60
40
20
Price ($/MWh)
Jan 6,1997
Jan 6,1998
Jan 6,1999
Dec 31,1999
Date

Figure 5

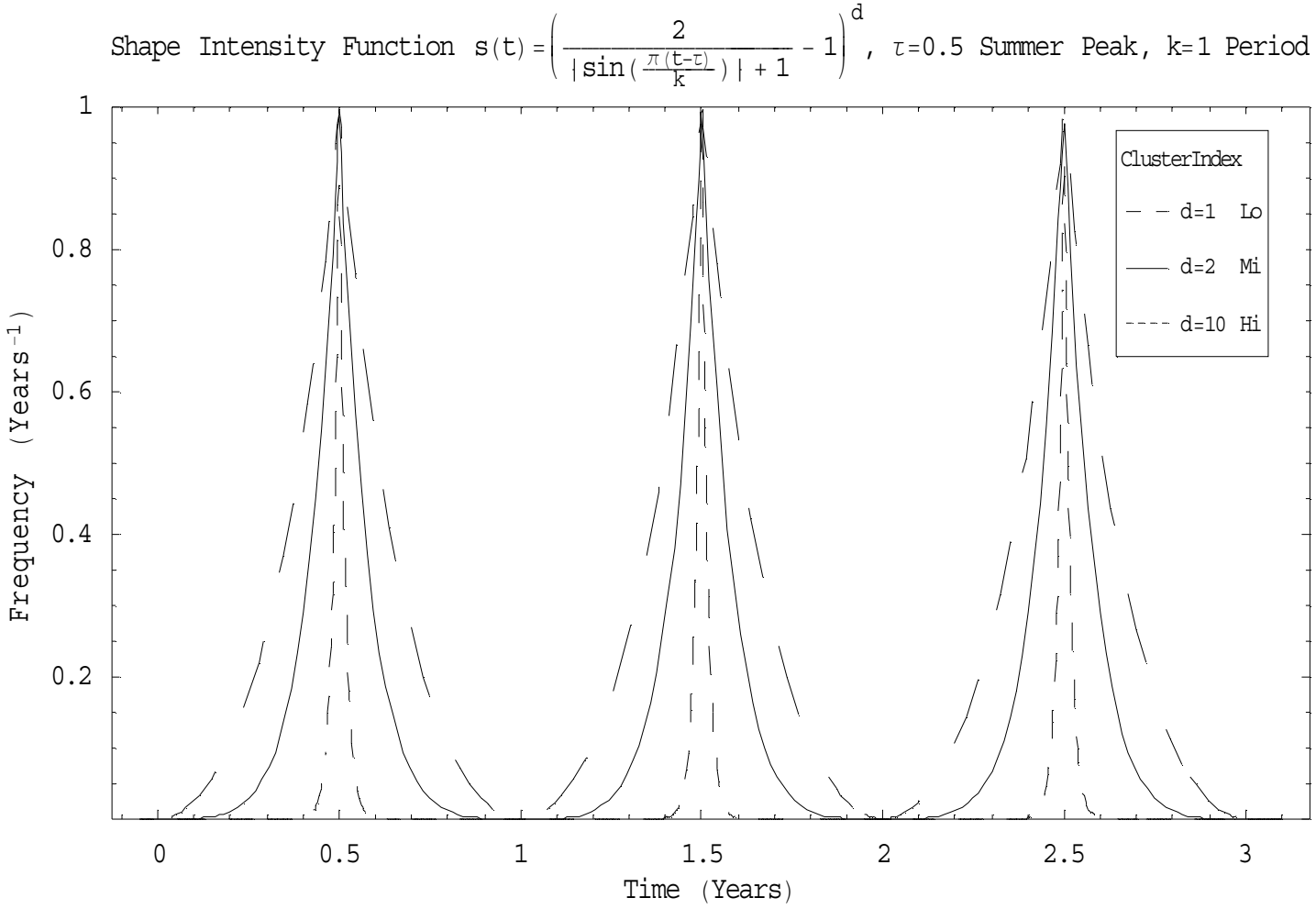
Shape Intensity Function $s(t)=\left(\frac{2}{|\sin(\frac{\pi(t-\tau)}{k})|+1}-1\right)^d$, τ=0.5 Summer Peak, k=1 Period
Frequency (Years^{-1})
1
0.8
0.6
0.4
0.2
0
0.5
1
1.5
2
2.5
3
Time (Years)
ClusterIndex
d=1 Lo
d=2 Mi
d=10 Hi

Figure 6

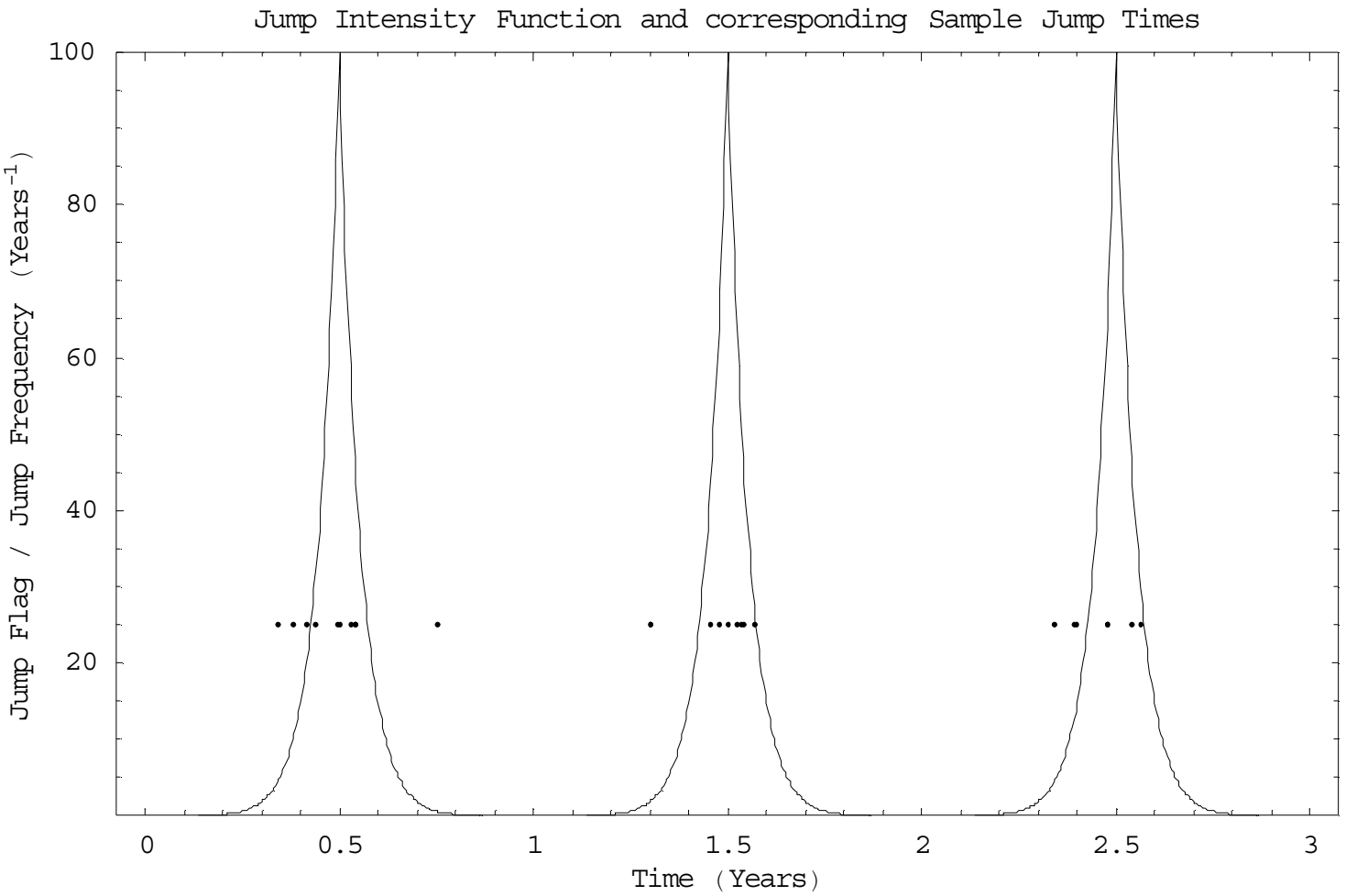
Jump Intensity Function and corresponding Sample Jump Times
Jump Flag / Jump Frequency (Years^{-1})
100
80
60
40
20
0
0.5
1
1.5
2
2.5
3
Time (Years)

Figure 7

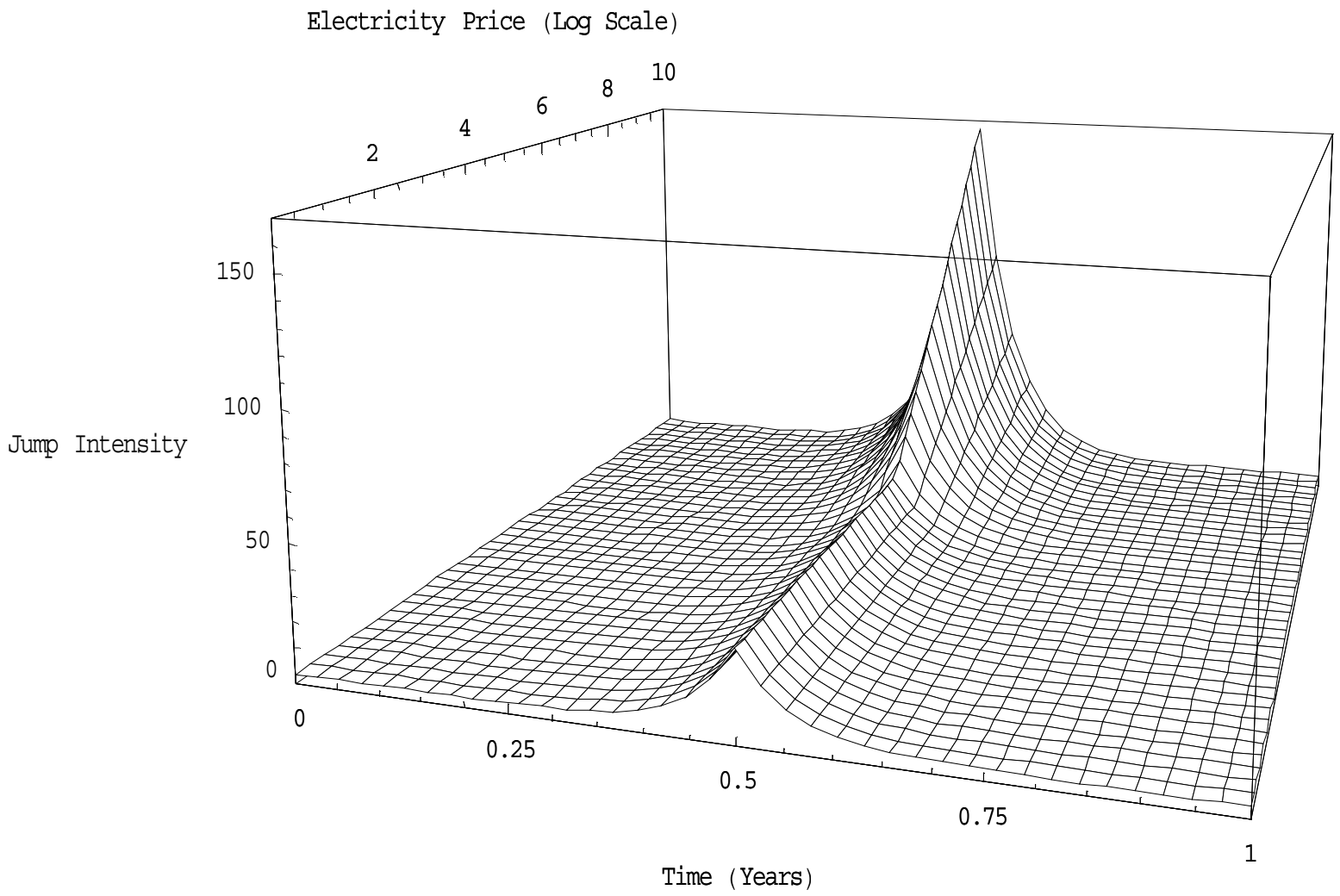
Electricity Price (Log Scale)
2
4
6
8
10
150
100
50
0
Jump Intensity
0
0.25
0.5
0.75
1
Time (Years)

Figure 8

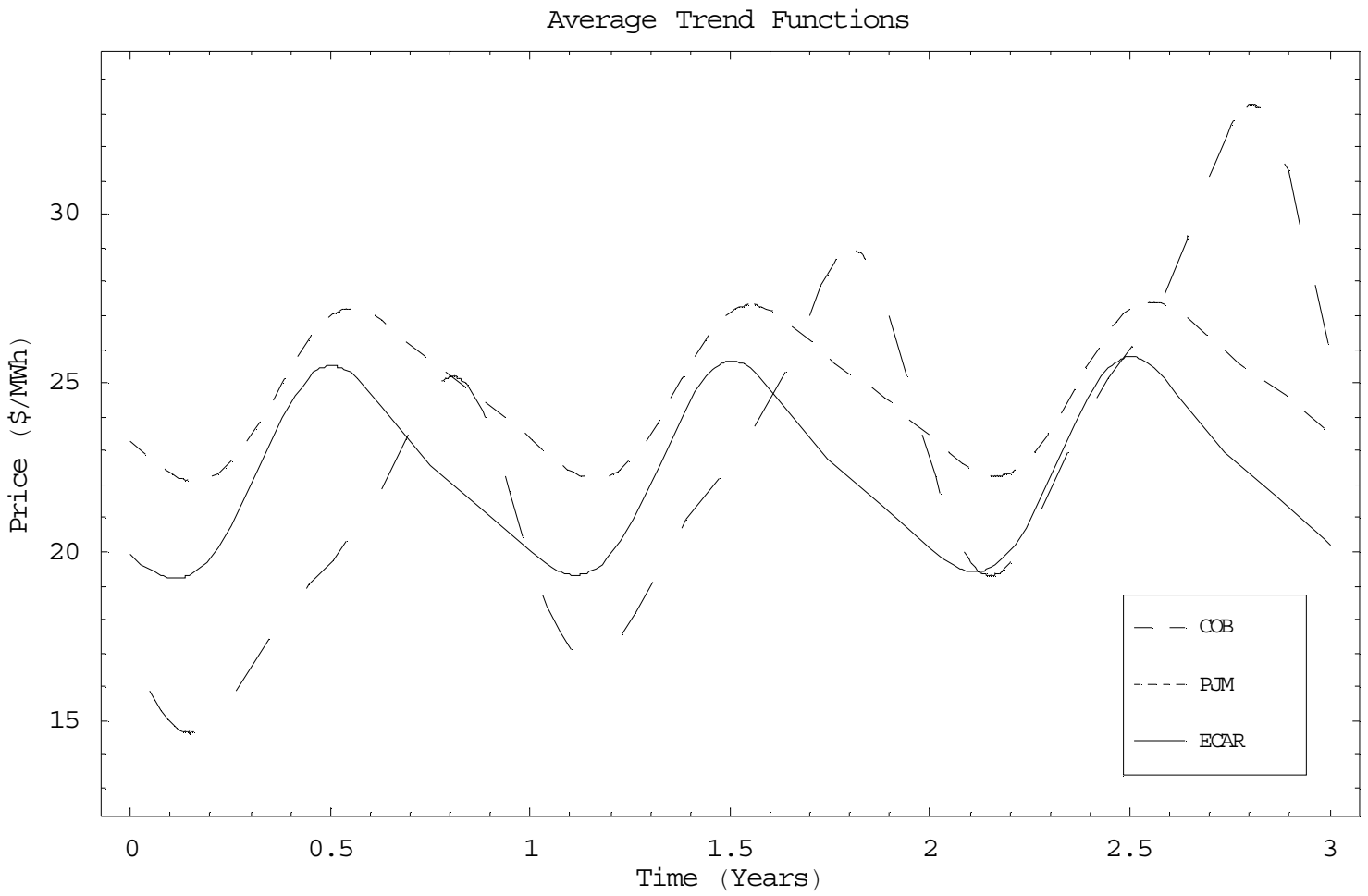
Average Trend Functions
Price ($/MWh)
30
25
20
15
0
0.5
1
1.5
2
2.5
3
Time (Years)
COB
PJM
ECAR

Figure 9

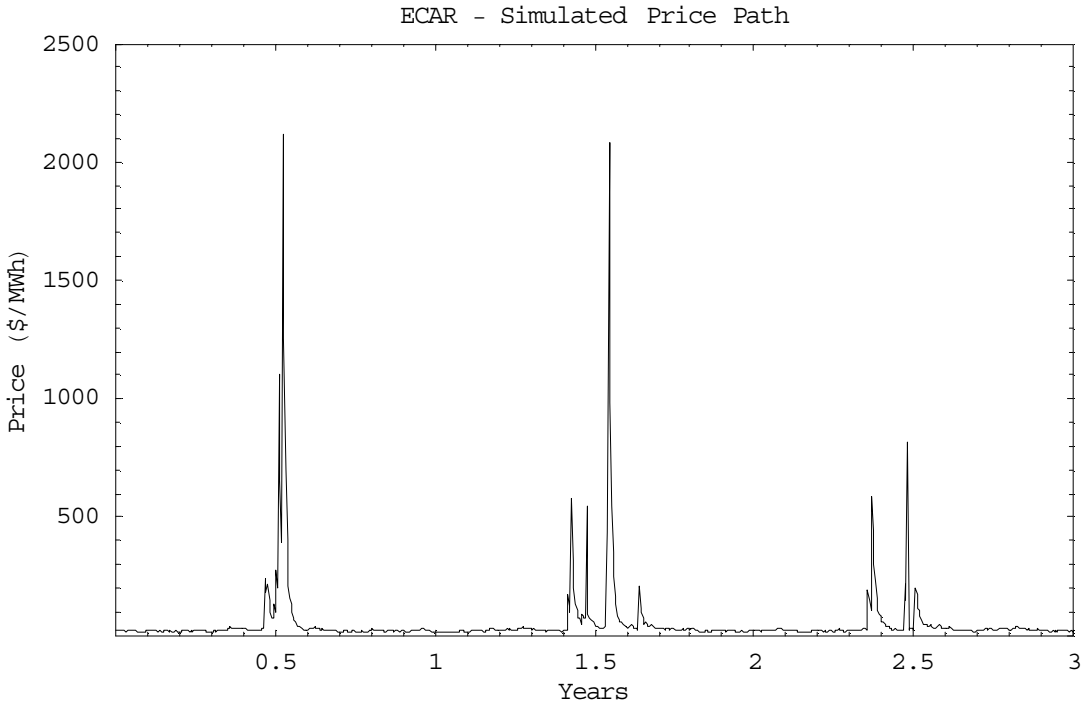
ECAR - Simulated Price Path
2500
2000
1500
1000
500
Price ($/MWh)
0.5
1
1.5
2
2.5
3
Years

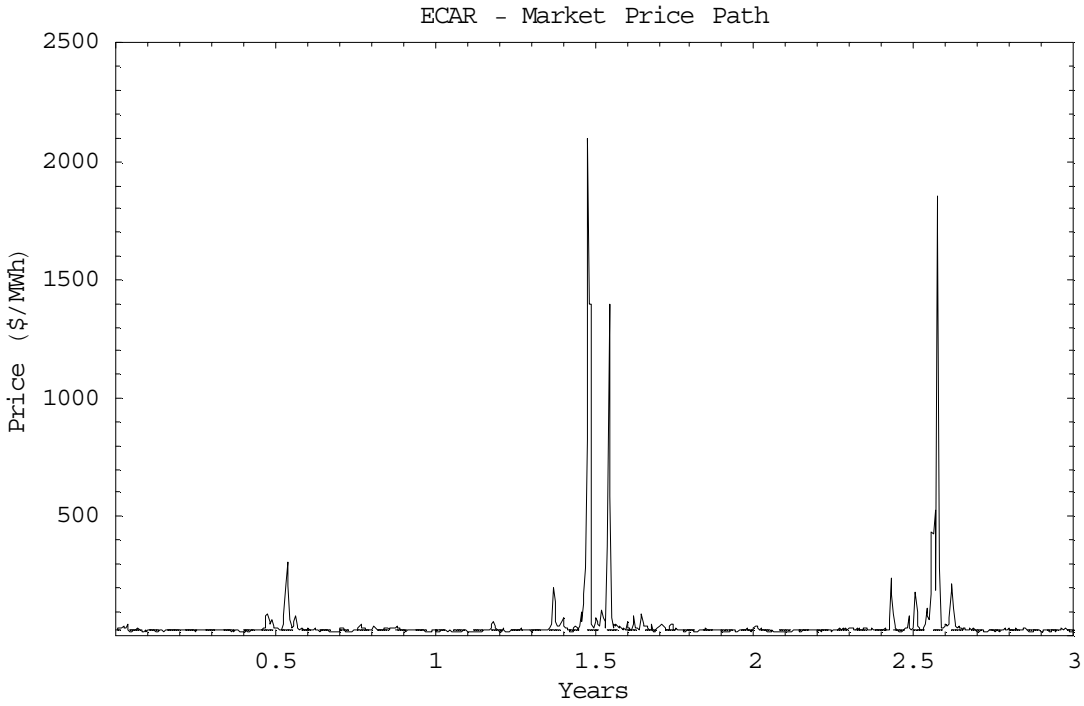
ECAR - Market Price Path
2500
2000
1500
1000
500
Price ($/MWh)
0.5
1
1.5
2
2.5
3
Years

Figure 10(a)

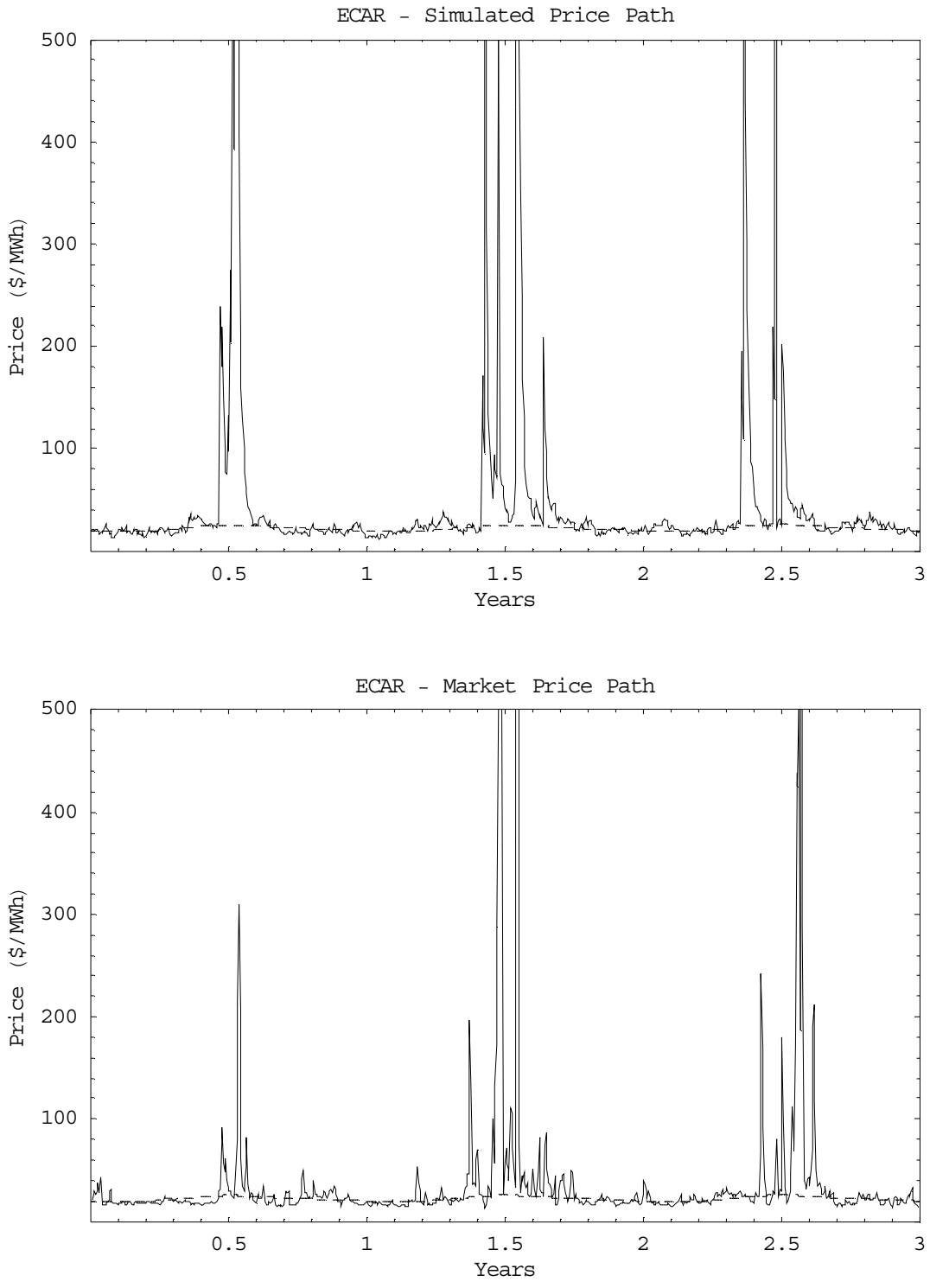
ECAR - Simulated Price Path
Price ($/MWh)
500
400
300
200
100
0.5
1
1.5
2
2.5
3
Years
ECAR - Market Price Path
Price ($/MWh)
500
400
300
200
100
0.5
1
1.5
2
2.5
3
Years

Figure 10(b)

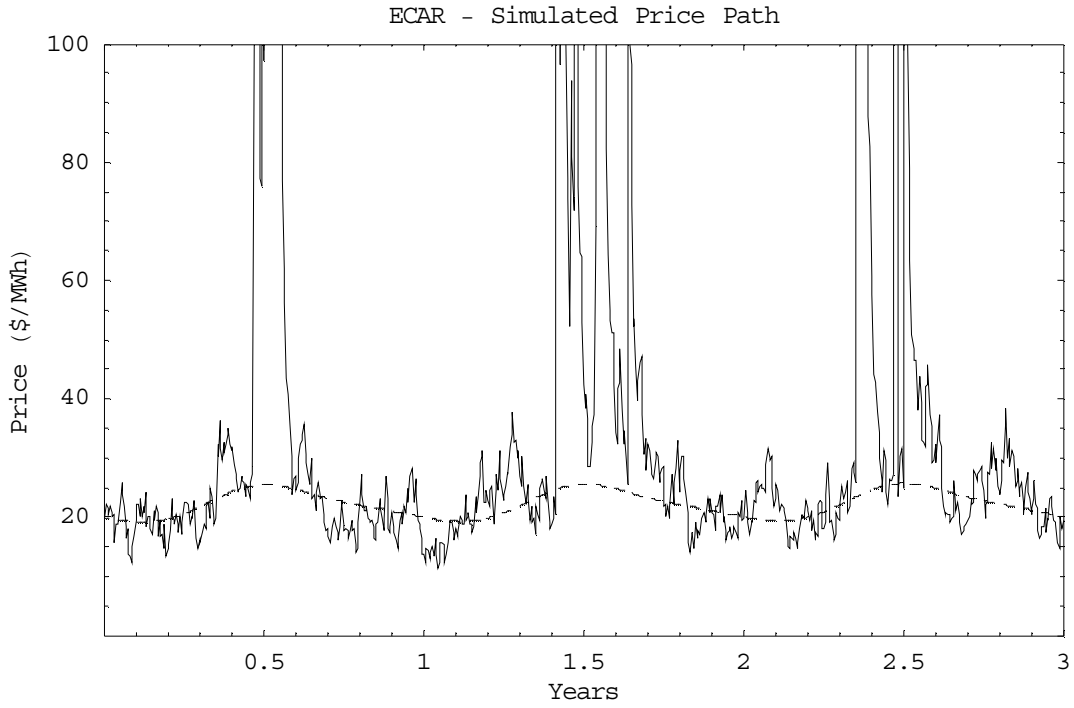
ECAR - Simulated Price Path
Price ($/MWh)
100
80
60
40
20
0.5
1
1.5
2
2.5
3
Years

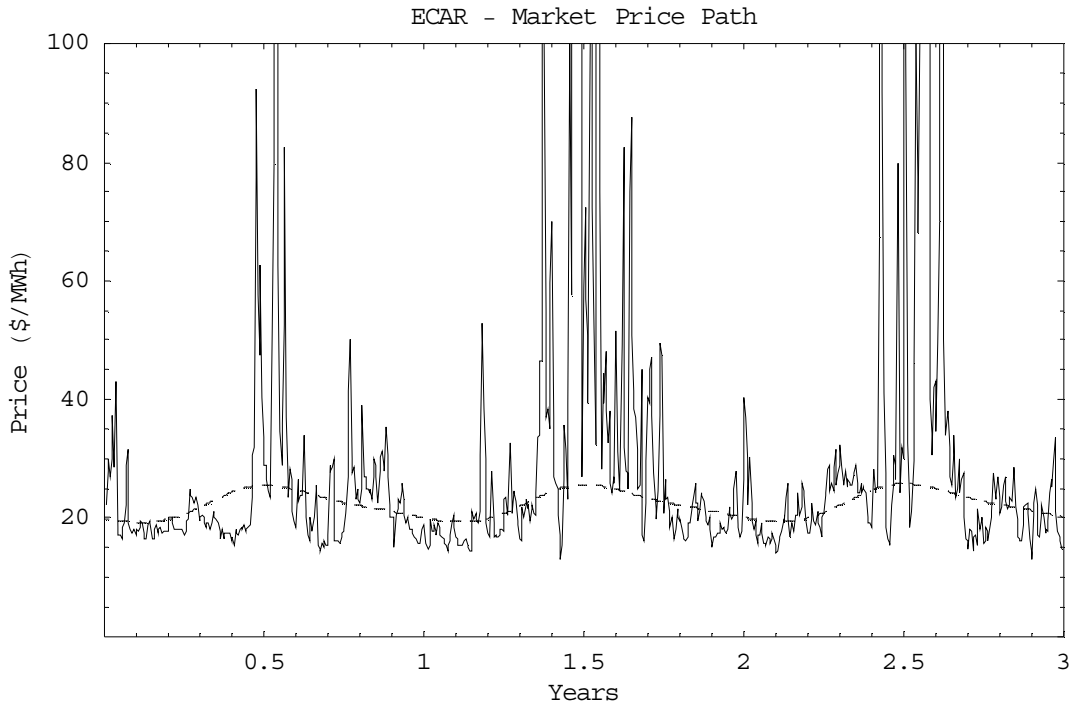
ECAR - Market Price Path
Price ($/MWh)
100
80
60
40
20
0.5
1
1.5
2
2.5
3
Years

Figure 10(c)

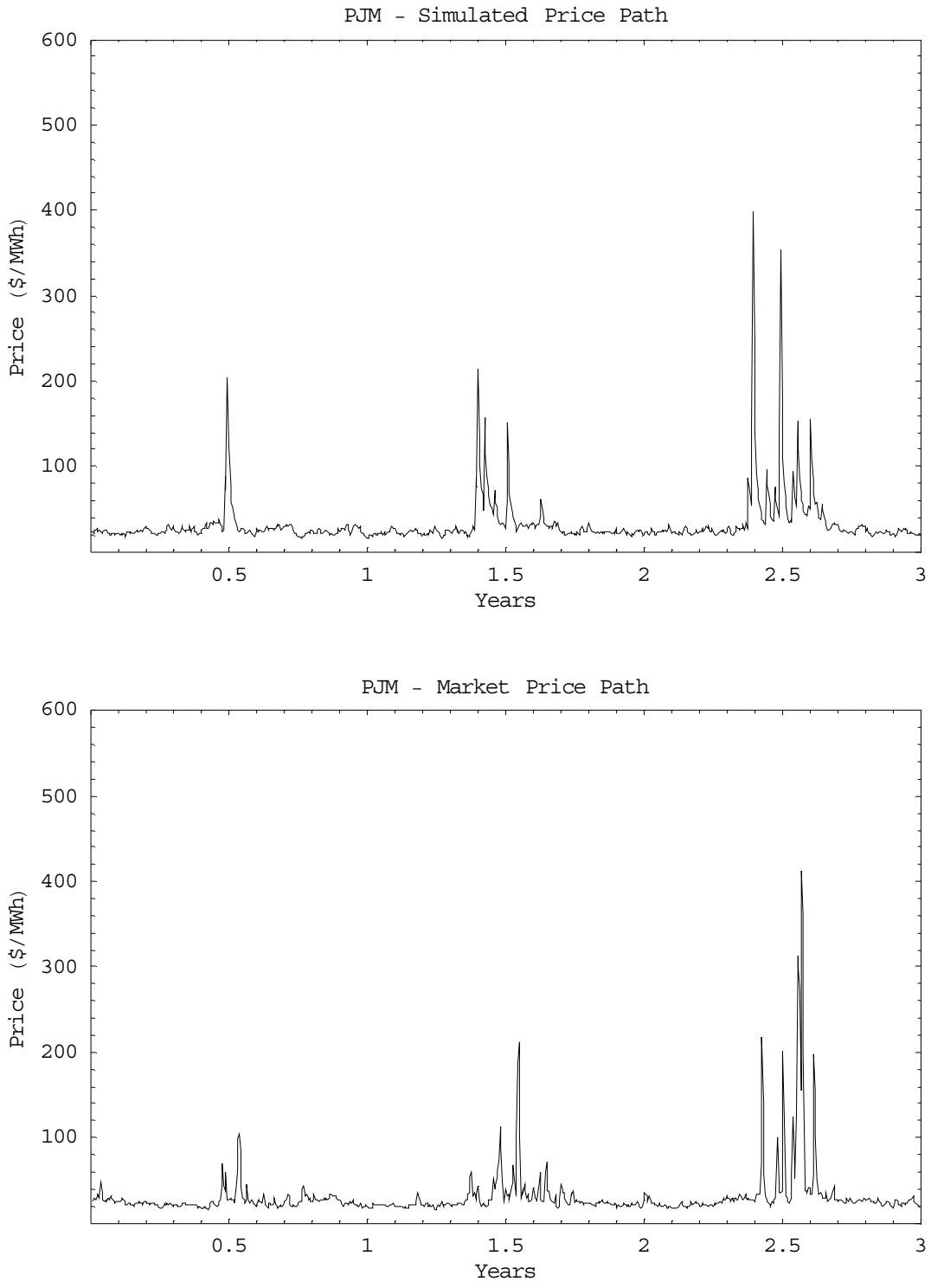
PJM - Simulated Price Path
Price ($/MWh)
600
500
400
300
200
100
0.5
1
1.5
2
2.5
3
Years
PJM - Market Price Path
Price ($/MWh)
600
500
400
300
200
100
0.5
1
1.5
2
2.5
3
Years

Figure 11(a)

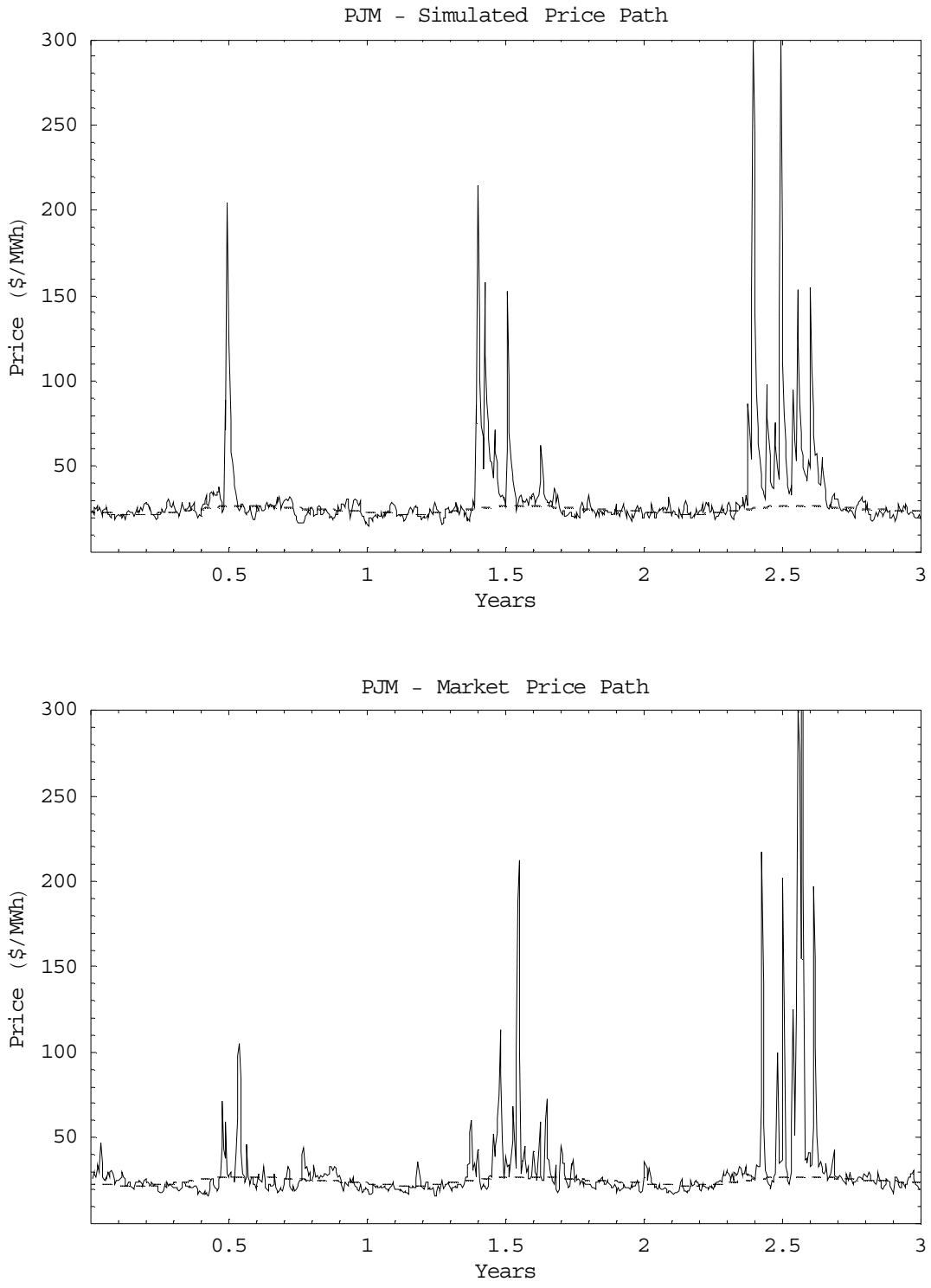
PJM - Simulated Price Path
Price ($/MWh)
300
250
200
150
100
50
0.5
1
1.5
2
2.5
3
Years
PJM - Market Price Path
Price ($/MWh)
300
250
200
150
100
50
0.5
1
1.5
2
2.5
3
Years

Figure 11(b)

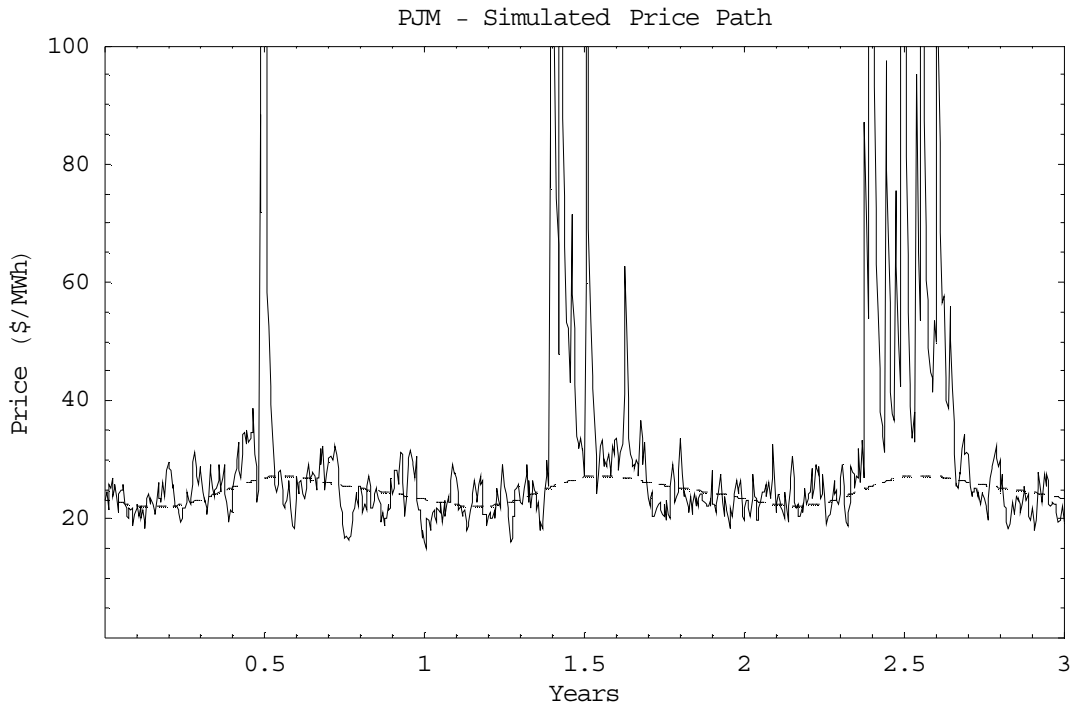
PJM - Simulated Price Path
Price ($/MWh)
100
80
60
40
20
0.5
1
1.5
2
2.5
3
Years

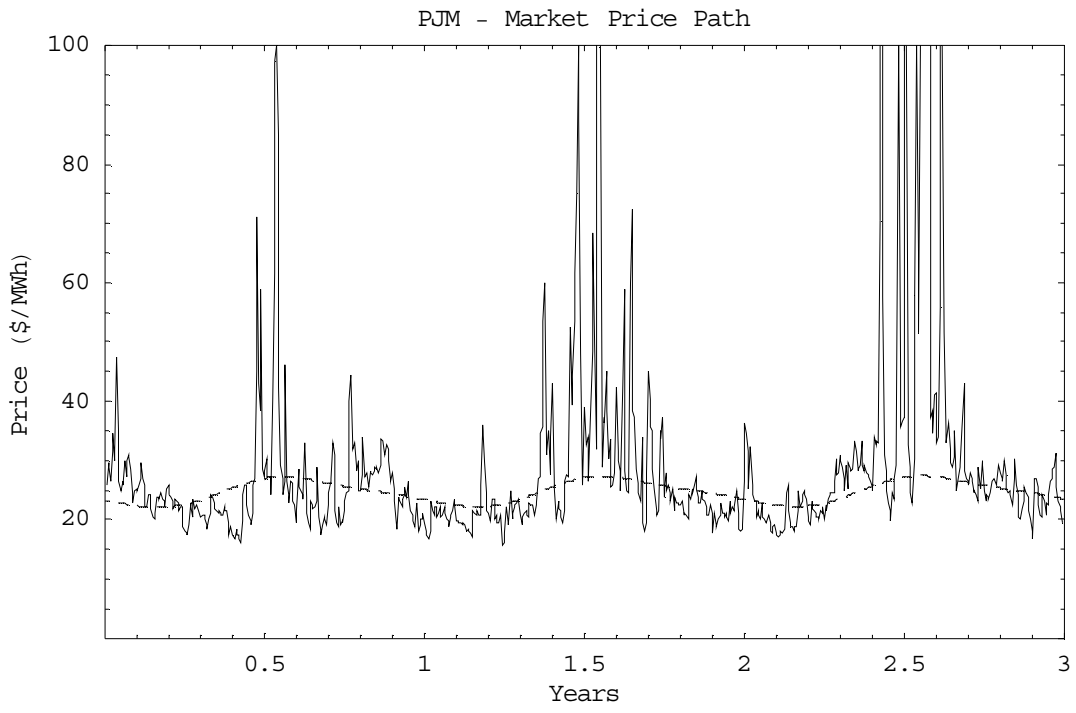
PJM - Market Price Path
Price ($/MWh)
100
80
60
40
20
0.5
1
1.5
2
2.5
3
Years

Figure 11(c)

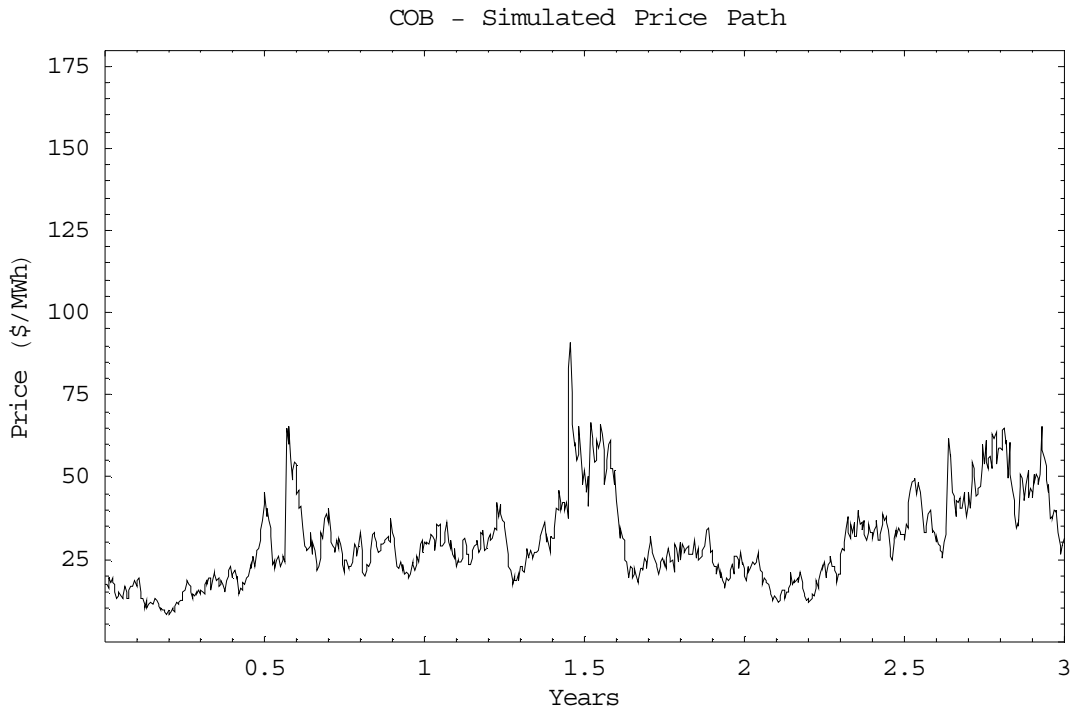
COB - Simulated Price Path
Price ($/MWh)
175
150
125
100
75
50
25
0.5
1
1.5
2
2.5
3
Years

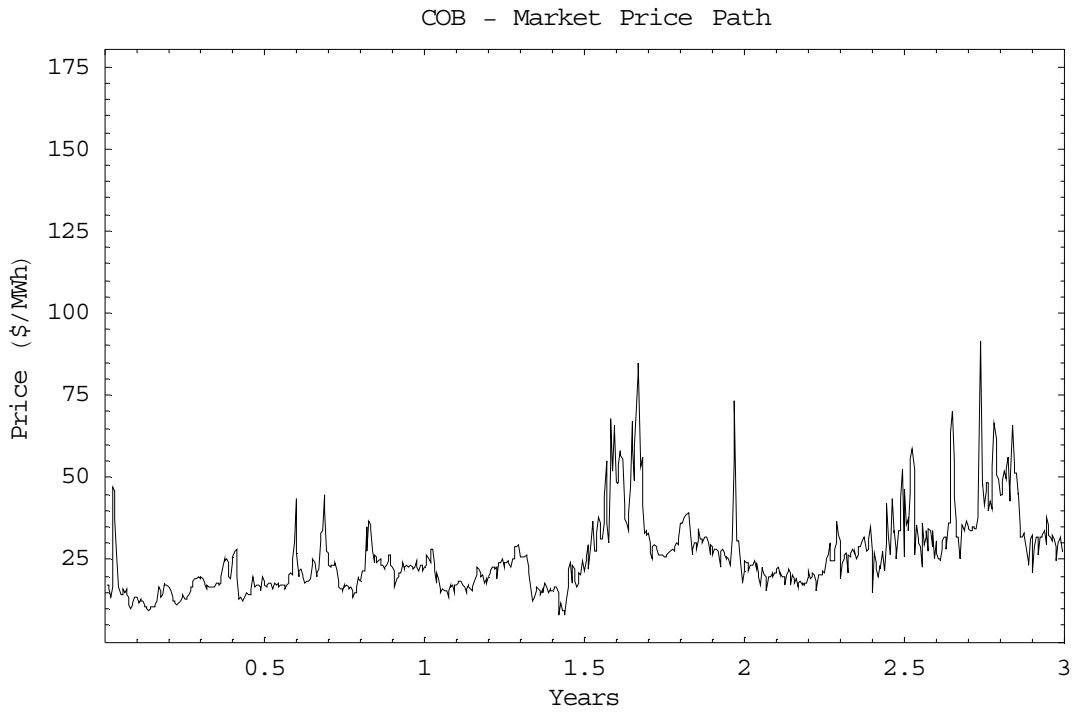
COB - Market Price Path
Price ($/MWh)
175
150
125
100
75
50
25
0.5
1
1.5
2
2.5
3
Years

Figure 12(a)

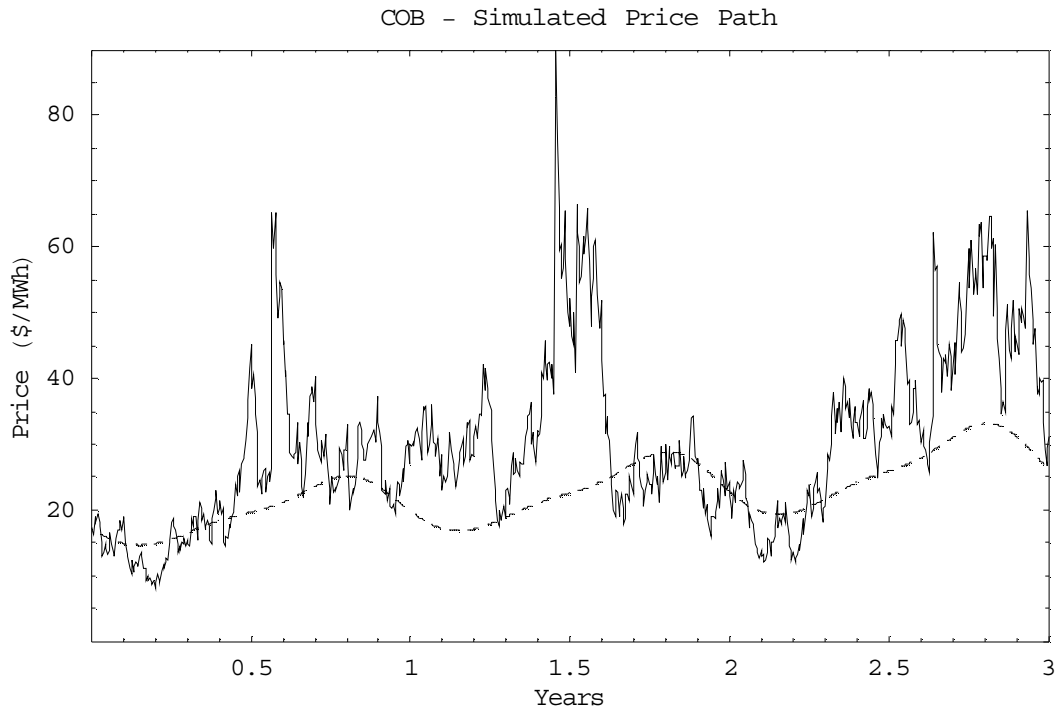
COB - Simulated Price Path
Price ($/MWh)
80
60
40
20
0.5
1
1.5
2
2.5
3
Years

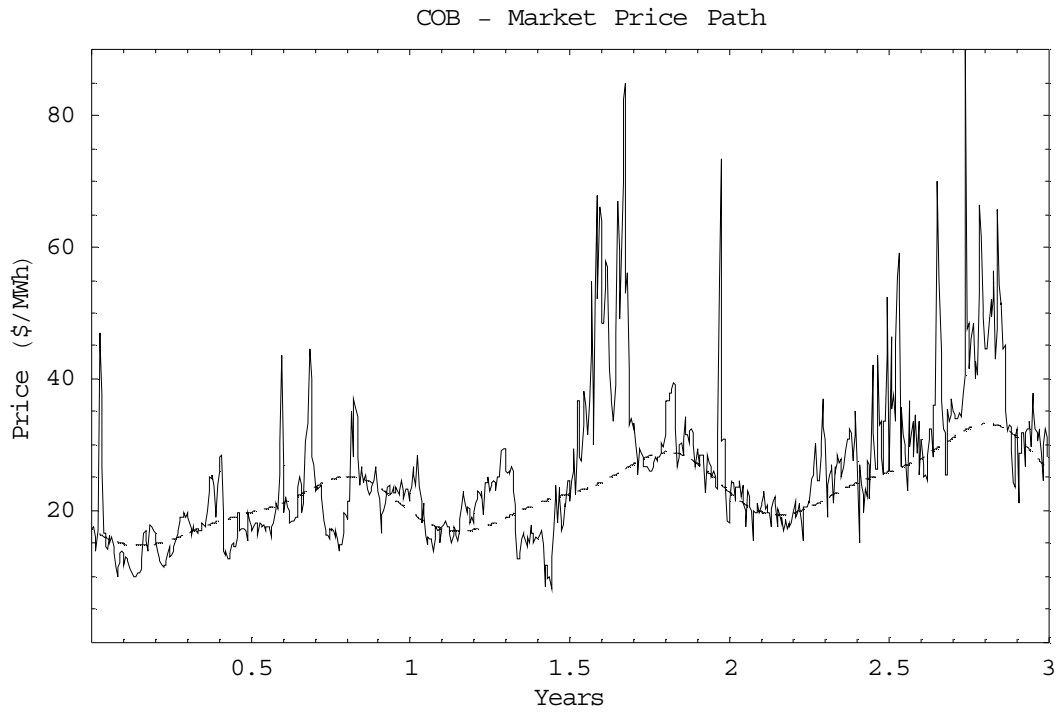
COB - Market Price Path
Price ($/MWh)
80
60
40
20
0.5
1
1.5
2
2.5
3
Years

Figure 12(b)

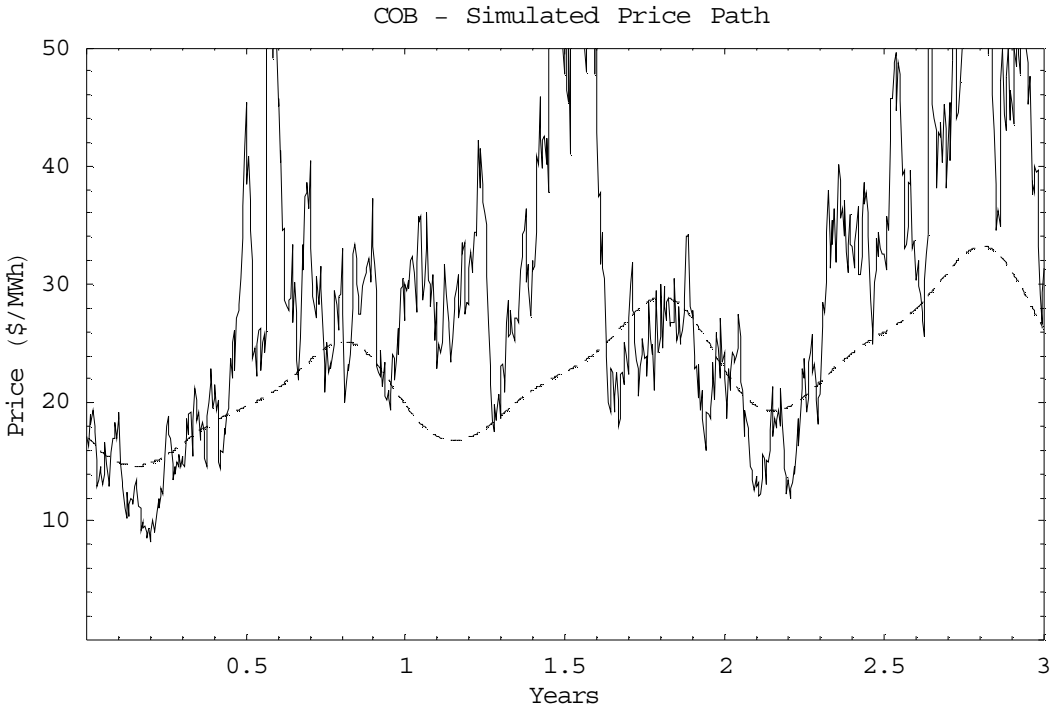
COB - Simulated Price Path
Price ($/MWh)
50
40
30
20
10
0.5
1
1.5
2
2.5
3
Years

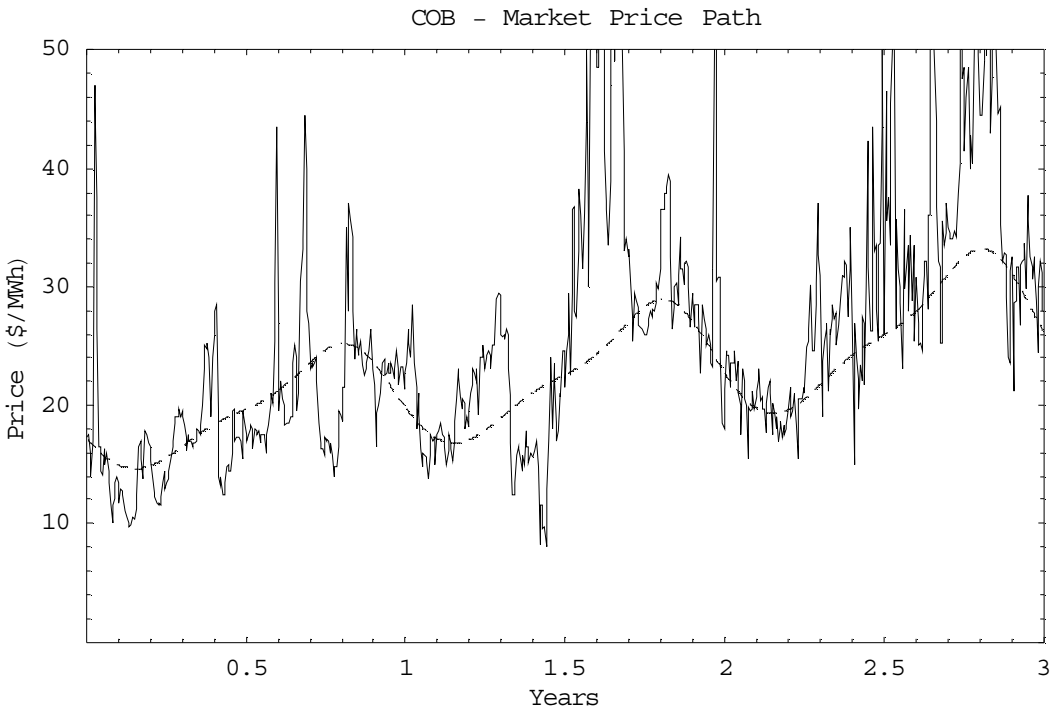
COB - Market Price Path
Price ($/MWh)
50
40
30
20
10
0.5
1
1.5
2
2.5
3
Years

Figure 12(c)